UNIVERSITY OF CALIFORNIA, IRVINE

Millimeter Waves in Single-Carrier Massive MIMO Transmissions

THESIS

Submitted in Partial Satisfaction of the Requirements For the

Degree of

MASTER OF SCIENCE THESIS

In Electrical and Computer Engineering

By

Nader P. BEIGI

Thesis Committee:

Professor Ender Ayanoglu, Chair

Professor Syed Ali Jafar

Professor Hamid Jafarkhani

2017

Dedication

Dedicated to my beloved family

Contents

List of Figures

List of Abbreviations

MU	**M**ulti **U**ser
MISO	**M**ultiple **I**nput **S**ingle **O**utput
GBC	**G**aussian **B**roadcast **C**hannel
MIMO	**M**ultiple **I**nput **M**ultiple **O**utput
BS	**B**ase **S**tation
PDP	**P**ower **D**elay **P**rofile
ISI	**I**nter **S**ymbol **I**nterference
MUI	**M**ulti **U**ser **I**nterference
OFDM	**O**rthogonal **F**requency **D**evision **M**ultiplexing
FIR	**F**inite **I**mpulse **R**sponse
IIR	**I**nfinite **I**mpulse **R**esponse
AWGN	**A**dditive **W**hite **G**aussian **N**oise
CSI	**C**hannel **S**tate **I**nformation
CIR	**C**hannel **I**mpulse **R**esponse
SNR	**S**ignal to **N**oise power **R**atio
PAPR	**P**eak to **A**verage **P**ower **R**atio
PAN	**P**ersonal **A**rea **N**etwork
LAN	**L**ocal **A**rea **N**etwork

Acknowledgements

Many thanks to my family, my mother, father, and brother who always support me. Thanks to my advisor, professor Ender Ayanoglu, who always show me the best way to be a researcher.

Also, I wish to express my special thanks to Gokhan Guvensen for his advice and suggestions.

ABSTRACT OF THE THESIS

Millimeter Waves in Single-Carrier Massive MIMO Transmissions

by

Nader P. Beigi

Master of Science in Electrical Engineering

University of California, Irvine, 2017

Professor Ender Ayanoglu, Chair

This work presents a single-carrier transmission for the frequency selective Gaussian multi-user channel. It considers both dependent and independent channel cases and compares them in terms of the user sum-rate as well as the general performance. We developed a general expression for the achievable rate among users in the channel with a particular type of correlation. In this channel, the conventional channel matched filter does not perform as expected. We applied three different precoders to enhance the performance. Their performances are determined by simulations.

We showed the superiority of the precoders with a large number of users through simulations. By increasing the number of users in the system, the conventional pre-coders showed better performance in terms of the user sum-rates. We showed that a correlation not only between antennas, but also between taps can affect the performance of the channel matched filter.

Chapter 1

Millimeter Waves

1.1 Introduction

A basic introduction for millimeter waves (mmW) is that their frequencies are between 30GHz and 300GHz. Millimeter waves are a new area for cellular communications that offer greater bandwidth and further gains via beamforming and spatial multiplexing from multi-element antenna arrays [3]. Since demand for cellular data has been increasing significantly during recent years with conservative estimates ranging from 40% to 70% increase in traffic each year [3], using millimeter waves can be a solution to the need to support it. This growth in demand for cellular data implies that within the next decades, there will be as much as 1000 times data that current levels of capacity can deliver. As a matter of fact, many new devices will require wireless services within the next decades due to the benefits of wireless connectivity move beyond smartphones, tablets, and other means of communications.

Using millimeter waves instead of current frequency bands can be a suggestion to answer growing demands for cellular data in the future. The available bandwidth in millimeter waves bands are much wider than today's cellular networks. The available spectrum at these higher frequencies can be two orders of magnitude greater than all cellular allocations today that are largely constrained to the Radio Frequency (RF) spectrum under 3GHz [3]. These tremendous potentials have led to noticeable increasing interest in millimeter waves both in industry and academia. There is a growing belief that millimeter waves will play a significant role in future cellular communications systems.

Despite the fact that other aspects of cellular mobile technology have been tremendously progressed since digital cellular systems have been considered as a major vehicle for communications, the carrier frequencies of those systems remain mainly the same. With today's severe shortage of spectrum, and because technology has reached the point of being able to support them, it will be very useful to unleash those frequencies that have not been considered before. However, it should be kept in mind that the development of millimeter waves in future cellular networks may still face some technical obstacles.

Due to the higher frequencies of millimeter wave transmissions, any increase in omnidirectional path loss can be completely compensated through directional transmission and beamforming. However, transmission through millimeter wave bands can result in outages and intermittent channel quality because signals in millimeter wave bandwidth can be vulnerable to shadowing. Also, power consumption by the user's device can be very high to support a large number of antennas with wide bandwidths. Other obstacles to millimeter waves cellular transmission are limited signal range for Non-Line-Of-Sight (NLOS) propagation and links with long distances. There are a large number of studies for indoor applications of millimeter waves, but the outdoor studies are relatively new [3].

1.2 History of Millimeter Waves

As it is mentioned before, millimeter wave signals refer to wavelengths from 1mm to 10mm, which corresponds to frequencies in the range of 30GHz to 300GHz. Wireless communications in millimeter wave bands is not new, the first millimeter communications were demonstrate more than 100 years ago [3]. Currently, millimeter wave bands are used mostly for satellite communications and cellular backhaul. Also, millimeter wave bands have been recently used for very hight throughput wireless LANs and personal area network systems in the unlicensed 60GHz band [3]. Most applications (even those new ones) are mostly for short range or point-to-point Line-Of-Sight (LOS) settings.

As it is mentioned before, the application of millimeter wave bands for longer range or NLOS cellular scenarios is a new field and the feasibility of such systems has been the subject of debate. Although millimeter wave spectrum offers greater bandwidth and more gains than current cellular communications network, there is a fear that the propagation of millimeter wave bands might not be as favorable as it is thought to be. Signals in millimeter wave bands suffer from shadowing, intermittent connectivity, and will have higher Doppler spreads. with these limitations in mind, there are considerable skepticisms that millimeter wave bands would be viable for cellular systems that require reliable communication across longer range and NLOS paths [3]. It should be noted that significant progress has been made in particular in power amplifiers and array combining, and these technologies can advance further with the growth of frequency range in wireless system.

1.3 Challenges Ahead

Despite all potentials and benefits of millimeter wave bands in cellular systems, there are a number of major challenges as we will discuss below.

1.3.1 Range and Directionality

It can be shown that the omnidirectional path loss in free space grows with the square of the frequency (Friis' transmission law [3]). Therefore, one might think that higher frequencies of millimeter wave bands can increase the propagation loss in free space. However, the smaller wavelength of millimeter wave signals can enable greater antenna gains for the same size of antennas. Thus, the frequencies of the signals in millimeter wave bands will not increase the propagation loss. Note that the reliance on highly directional transmissions might need certain changes in design of the current cellular systems [3].

1.3.2 Shadowing Effect

As it is mentioned before, one of the major concerns is millimeter wave signals are extremely vulnerable to shadowing. For example, human bodies can result in 20dB to 35dB loss. One might think because signals in the millimeter wave bands are susceptible to shadowing, usage of these signals is not practical. However, one can see the human body and other obstacles resulting shadowing and their reflective nature as a main source of scattering for millimeter wave propagation. Also, humidity and rain fades, the most common issues for the long range millimeter wave backhaul links, are not a problem in cellular systems [3].

1.3.3 Intermittent Connectivity

Due to the higher frequencies of millimeter wave signals, Doppler effect will be much faster than today's cellular systems. As we know, channel coherence time is linear in the carrier frequency for a given mobile velocity. This means that coherence time in the millimeter wave range is very small and the channel changes faster than today's cellular systems. Also, appearance of the obstacles will lead to more swings in path loss due to the high levels of shadowing. However, beamforming can resolve this issue and in addition, millimeter wave systems will be built for smaller cell size than today's [3]. This means that relative path loss and cell association will also change rapidly. Therefore, communication will need to be rapidly adoptable for the future cellular systems.

1.3.4 Multiuser Coordination

As it is mentioned before, current application of millimeter wave transmission are mostly focused on point-to-point or local links (such as LAN and PAN system) with limited number of users. New mechanisms will be needed to coordinate simultaneous transmissions on multiple interfering links to achieve high spatial reuse and spectral efficiency in cellular systems.

1.3.5 Power Consumption

Another key challenge of millimeter wave bands is that in order to increase the gains of antenna arrays, wide bandwidth of the millimeter wave signal consumes a lot of power in the A/D conversion. Note that power consumption scales linearly in the sampling rate and exponentially in the number of bits per each sample [3]. This makes high-resolution quantization at side bandwidths and large number of antennas prohibitive for low-power and low-cost devices.

Also, for phased array antennas, efficient RF power amplification and combining will be needed [3].

1.4 Conclusion

Future wireless networks will have bandwidths centered on carrier frequencies larger than 10GHz [4]. One can say despite the large path loss, millimeter wave frequencies can be successfully used to transmit large data-rate over short distances or slow-moving users (due to the distance and Doppler effects as we discussed before).

Millimeter wave bands systems have tremendous potentials and using them in cellular networks can lead to surprising benefits such as greater spectrum and further gains from high dimensional antenna arrays. However, as we mentioned in this chapter, millimeter wave cellular systems may need to be significantly redesigned to obtain the full potentials of millimeter wave bands. Reliance on directional transmissions and beamforming lead to reconsideration of many aspects of current cellular systems [3].

In addition, interference mitigation has been dominant in new cellular technologies in the past few decades. This might have a less significant impact on millimeter wave systems due to the directional isolation between links. On the other hand, technologies such as carrier aggregation and multihop relaying which have modest benefits in current cellular networks can play significant roles in the millimeter wave space [3].

During next chapters, we will show some millimeter wave applications on ideal and real channels and see the quality of the performance of millimeter wave signals in an environment of noise and interference.

Chapter 2

Independent AWGN Channel

2.1 Introduction

We begin by the description of what we mean by the independent channel. It is a frequency-selective multiple-user, multiple-input, multiple-output (MU-MIMO) downlink channel, with M base station antennas and K single antenna users. Independent channel here means different delay components, users, and base station antennas are independent from each other. By using the term independent, we do not mean that these different components have no interference on each other. Later on, we will see how they interfere with one another and discuss how to deal with it. The development we will provide in this chapter is based on [1], however, we will discuss some of the derivation in [1] in more detail here.

The channel between the m-th transmit antenna and the k-th user can be modeled as a finite impulse response (FIR) filter with L taps. The L taps correspond to different delay components. The l-th channel tap can be written as $\sqrt{d_l[k]}h_l^*[m,k]$ where $d_l[k]$ and $h_l^*[m,k]$ correspond to the slow-varying and fast-varying components of the channel, respectively. The variables $d_l[k]$'s represent the Power Delay Profile (PDP) of the frequency-selective channel. We assume that the slow-varying component, i.e., $\sqrt{d_l[k]}$ is fixed (as it is assumed in [1]). When we say the channel is independent, we mean the matrix of the fast-varying components of the channel has independent and identically distributed (i.i.d.) elements (i.e., $h_l^*[m,k]$'s are i.i.d. and they are fixed during the transmission of N symbols).

We know in the case that the channel is independent (for users, taps, and base station antennas), the channel matched filter is the best option to use. With this in mind, the channel matched filter can recover the desired signal out of the received one while maximizing the output Signal-to-Noise Ratio (SNR) in the presence of Additive White Gaussian Noise (AWGN). We also assume the independent channel has AWGN at each receive antenna.

2.2 Channel Matched Filter

We will now describe the system model in more detail. The transmitted symbols from base station antennas could be sent out without any preprocessing. But here we choose to use the optimum precoder, which is actually the channel matched filter. We note the difference with the common use of the channel matched filter in that we place it on the transmitter, not the receiver side. As we will show, as long as the channel is independent from taps, users, and base station antennas, the channel matched filter will perform in an optimum manner.

2.2.1 System Model

We now describe the system model in detail. Assume $x_m[i]$ is the symbol transmitted from transmit antenna m at time i, and $y_k[i]$ is the signal that the k-th user receives at time i. The received signal will be obtained after the convolution of the transmitted signal with the channel and AWGN and can be written as

$$y_k[i] = \sum_{l=0}^{L-1} \sum_{m=1}^{M} \sqrt{d_l[k]} h_l^*[m,k] x_m[i-l] + n_k[i], \tag{1}$$

where $n_k[i]$ is the $\mathcal{CN}(0,1)$ distributed AWGN at the k-th user and at time i. The channel PDP for each user is normalized such that

$$\sum_{l=0}^{L-1} d_l[k] = 1, \forall k = 1, \cdots, K. \tag{2}$$

The channel PDP possesses the distribution of the received power across different channel taps. The base station is assumed to have full Channel State Information (CSI), whereas the users only have knowledge of the channel statistics. We can express (2.1) in matrix format. This will enable more compact notation and simplicity in the sequel. First, we need to define $\vec{y}[i] \triangleq [y_1[i], \cdots, y_K[i]]^T \in \mathbb{C}^K$ and $\vec{x}[i] \triangleq [x_1[i], \cdots, x_M[i]]^T \in \mathbb{C}^M$ as the vector of received user symbols and the vector of transmitted symbols at time i, respectively. Let $\vec{n}[i] \triangleq [n_1[i], \cdots, n_K[i]]^T$ be AWGN with independent components (we assume it has Gaussian distribution). We also need to define $\mathbf{D}_l \triangleq \mathrm{diag}\{d_l[1], \cdots, d_L[k]\}$, and $\mathbf{H}_l \in \mathbb{C}^{M\times K}$ which is a matrix whose $[m,k]$-th element is $h_l[m,k]$. With all of these in mind, the received signal vector at time i can be written as

$$\vec{y}[i] = \sum_{l=0}^{L-1} \mathbf{D}_l^{\frac{1}{2}} \mathbf{H}_l^H \vec{x}[i-l] + \vec{n}[i]. \tag{3}$$

We can use different techniques to build the transmitted symbol. We can send the symbol out all by its own, without any equalization or pre-coder. However, in this section we will employ the channel matched filter as the precoder and we will analyze its performance. So let's say $s_k[i]$ is the information symbol to be communicated to the k-th user at time i. We will use the vector form for information symbols such that $\vec{s}[i] \triangleq [s_1[i], \cdots, s_K[i]]^T$ and it is considered to have independent and identically distributed $\mathcal{CN}(0,1)$ components. In other words, $\mathbb{E}[\vec{s}[i]\vec{s}^H[i+j]] = \mathbf{I}_K\delta_j$, and $\mathbb{E}[\vec{s}[i]\vec{s}^T[i+j]] = 0$ (correlation between transmit symbols at time i and $i+j$). As we mentioned before and it is stated in [1], in this chapter we consider the matched filter precoding scheme, where the transmitted vector at time i is given by

$$\vec{x}[i] = \sqrt{\frac{\rho_f}{MK}} \sum_{l=0}^{L-1} \mathbf{H}_l \mathbf{D}_l^{\frac{1}{2}} \vec{s}[i+l], \tag{4}$$

in which $\rho_f = \mathbb{E}[\|\vec{x}[i]\|^2]$ is actually the long-term average total power radiated by the base station antennas.

Proof. To prove that $\rho_f = \mathbb{E}[\|\vec{x}[i]\|^2]$ we need to calculate an expectation of (2.4) over $\vec{s}[i]$. So

$$\mathbb{E}\big[\|\vec{x}[i]\|^2\big] = \frac{\rho_f}{MK} \times \mathbb{E}\Bigg[\sum_{l'=0}^{L-1} \vec{s}^H[i+l']\mathbf{D}_{l'}^{\frac{1}{2}} \mathbf{H}_{l'}^H \sum_{l=0}^{L-1} \mathbf{H}_l \mathbf{D}_l^{\frac{1}{2}} \vec{s}[i+l]\Bigg]. \tag{5}$$

To calculate (2.5), we consider two cases where $l \neq l'$ or $l = l'$. With independent and identically distributed complex normal entries in $\mathbf{H}_l$, the value of the expectation in (2.5) is zero when $l \neq l'$. So we only need to consider the case that $l = l'$ in which case (2.5) can be written as

$$\mathbb{E}\big[\|\vec{x}[i]\|^2\big] = \frac{\rho_f}{MK} \times \mathbb{E}\Bigg[\sum_{l}^{L-1} \vec{s}^H[i+l]\mathbf{D}_l^{\frac{1}{2}} \mathbf{H}_l^H \mathbf{H}_l \mathbf{D}_l^{\frac{1}{2}} \vec{s}[i+l]\Bigg]. \tag{6}$$

For fixed K, we can show that as $M \to \infty$ the value $\mathbf{H}_l^H \mathbf{H}_l \to M \times \mathbf{I}_K$. So we can rewrite (2.6) as

$$\begin{aligned}
\mathbb{E}\big[\|\vec{x}[i]\|^2\big] &= \frac{\rho_f}{K} \times \mathbb{E}\big[\sum_{l=0}^{L-1} \vec{s}^H[i+l]\mathbf{D}_l \vec{s}[i+l]\big] \\
&= \frac{\rho_f}{K} \times \mathbb{E}\Big[\sum_{l=0}^{L-1}\sum_{q=1}^{K} \big|\vec{s}_q[i+l]\big|^2 \sqrt{d_l[q]}\Big] \qquad (7) \\
&= \frac{\rho_f}{K} \sum_{l=0}^{L-1}\sum_{q=1}^{K} \mathbb{E}\big[\big|\vec{s}_q[i+l]\big|^2\big] \sqrt{d_l[q]}.
\end{aligned}$$

Using (2.2) and the fact that information symbols are $\mathcal{CN}(0,1)$ we have

$$\mathbb{E}\big[\|\vec{x}[i]\|^2\big] = \frac{\rho_f}{K} \times \sum_{q=1}^{K} 1 = \rho_f. \qquad (8)$$

As a result, the average of the transmitted signal power is equal to ρ_f. ■

Later on, we will use this ρ_f to simulate the channel with different signal power.

2.2.2 Desired Signal and Effective Noise

First, we define $\vec{v}_l[k] \triangleq \mathbf{H}_l \mathbf{D}_l^{1/2} \vec{e}_k$, in which $\vec{e}_k$ is the vector with all of its elements equal to 0 except the k-th element which is equal to 1. It is going to be used to make the matrix format of our equations simpler. Now we can use (2.3) and (2.4) to rewrite the signal received by the user k at time i. As a result, $y_k[i]$ is given as

$$y_k[i] = \underbrace{\sqrt{\frac{\rho_f}{MK}}\Big(\sum_{l=0}^{L-1} \mathbb{E}\big[\vec{v}_l^H[k]\vec{v}_l[k]\big]\Big) s_k[i]}_{\text{Desired Signal Term}} + \underbrace{n'_k[i]}_{\text{Effective Noise Term}}, \qquad (9)$$

where $n'_k[i]$ is the actual effective noise term and can be written as [1]

$$
\begin{aligned}
n'_k[i] = & \underbrace{\sqrt{\frac{\rho_f}{MK}} \sum_{l=0}^{L-1} \left(\vec{v}_l^H[k]\vec{v}_l[k] - \mathbb{E}[\vec{v}_l^H[k]\vec{v}_l[k]] \right) s_k[i]}_{\text{Additional Interference Term (IF)}} \\
& + \underbrace{\sqrt{\frac{\rho_f}{MK}} \sum_{\substack{a=1-L \\ a\neq 0}}^{L-1} \sum_{l=\max(a,0)}^{\min(L-1+a,L-1)} \vec{v}_l^H[k]\vec{v}_{l-a}[k]s_k[i-a]}_{\text{Inter-Symbol Interference (ISI)}} \\
& + \underbrace{\sqrt{\frac{\rho_f}{MK}} \sum_{\substack{q=1 \\ q\neq k}}^{K} \sum_{a=1-L}^{L-1} \sum_{l=\max(a,0)}^{\min(L-1+a,L-1)} \vec{v}_l^H[k]\vec{v}_{l-a}[q]s_q[i-a]}_{\text{Multi-User Interference (MUI)}} \\
& + \underbrace{n_k[i]}_{\text{AWGN}} .
\end{aligned}
\tag{10}
$$

The effective noise term includes four different parts, (i) the additional interference (IF) term that we acquired by splitting the coefficient of the term $\sqrt{\frac{\rho_f}{MK}} \sum_{l=0}^{L-1} \vec{v}_l^H[k]\vec{v}_l[k]s_k[i]$ into a sum of its mean value (which is known to the receiver) and the deviation around its mean (hence, this term represents the variation of the desired signal around its mean), (ii) the Intersymbol Interference (ISI) term between the current symbol of the user k and symbols intended to the same users at other time instances (i.e., $s_k[i+j], j \neq 0$), (iii) the Multiuser Interference (MUI) term from other information symbols intended for other users, and (iv) AWGN of the channel. All these interference terms in the effective noise show that the effective noise is no longer Gaussian.

2.3 Sum-Rate of the Users

In the general case, the variance of the effective noise depends on the channel realization and the channel statistics. We assume codewords are long enough to make the effective noise variance independent from a particular channel realization and only dependent on channel statistics. With this assumption, the desired signal will be uncorrelated with the effective noise $n'_k[i]$ which means $\mathbb{E}\big[s_k[i]n'_k[i]\big] = 0$ (the expectation is taken over channel realization, the information symbols, and additive noise). Together with the assumption that we made (long enough codewords) that the noise in the channel is effectively additive non-Gaussian and uncorrelated with the information symbols (i.e., $s_k[i]$).

2.3.1 Noise and the PDP

With all that we mentioned before and assuming that the user has the perfect knowledge of its channel statistics (it means the user knows the scaling factor, i.e., $\sum_{l=0}^{L-1} \mathbb{E}\big[\vec{v}_l^H[k]\vec{v}_L[k]\big]$), we can say we will try to compute the achievable rate by considering the worst case in the channel. Given that the data signal $s_k[i]$ is Gaussian, the worst uncorrelated additive noise is circularly symmetric Gaussian distributed with the same variance as the effective noise, i.e., $n'_k[i]$ [1]. Hence, we can use the following expression to compute the achievable rate for the k-th receiver (user)

$$R_k = \log_2\big(1 + S_k/\mathrm{Var}(n'_k[i])\big), \tag{11}$$

where S_k is the average power of the desired signal term and can be calculated by

$$S_k = \mathbb{E}_{s_k[i]}\left[\left|\sqrt{\frac{\rho_f}{MK}}\sum_{l=0}^{L-1}\mathbb{E}\big[\vec{v}_l^H[k]\vec{v}_l[k]\big]\,s_k[i]\right|^2\right]. \tag{12}$$

Also the term $n'_k[i]$ is the effective noise variance and can be computed by

$$\mathrm{Var}(n'_k[i]) \triangleq \mathbb{E}\left[\left|n'_k[i] - \mathbb{E}\big[n'_k[i]\big]\right|^2\right]. \tag{13}$$

Both of the equations above are acquired from (2.9). Note that the effective noise variance is invariant of any channel PDP that satisfies (2.2). With this in mind, we can compute the effective noise variance as

$$\mathrm{Var}(n'_k[i]) = \rho_f + 1. \tag{14}$$

Proof. Using the expanded version of the effective noise variance which is provided in (2.10), we can rewrite the effective noise variance as

$$\begin{aligned}\mathrm{Var}(n'_k[i]) = \frac{\rho_f}{K}\sum_{q=1}^{K}\sum_{a=1}^{L-1}\sum_{l=a}^{L-1}\big(d_{l-a}[k]d_l[q] + d_l[k]d_{l-a}[q]\big) \\ + \frac{\rho_f}{K}\sum_{q=1}^{K}\sum_{l=0}^{L-1}\big(d_l[k]d_l[q]\big) + 1,\end{aligned} \tag{15}$$

where the expectation is taken over the statistics of the channel realization (here only $\mathbf{H}_l$), data symbols (i.e., $s_k[i+a]$), and the additive white Gaussian noise (i.e., $n_k[i]$). As it is exactly stated in [1], we define $\boldsymbol{\Delta} \in \mathbb{R}^{K\times L}$ such that $[\boldsymbol{\Delta}]_{i,j} = d_{j-1}[i]$ and $\mathbf{E} \in \{1\}^{L\times L}$ denotes the matrix with all entries equal to 1. Then, we can rewrite (2.16) as

$$\begin{aligned}\mathrm{Var}(n'_k[i]) = \frac{\rho_f}{K}\sum_{q=1}^{K}\sum_{a=1}^{L-1}\sum_{l=a}^{L-1}\vec{e}_k^{T}\boldsymbol{\Delta}\big(\vec{e}_{l-a+1}\vec{e}_{l=1}^{T} + \vec{e}_{l+1}\vec{e}_{l-a+1}^{T}\big)\boldsymbol{\Delta}^T\vec{e}_q \\ + \frac{\rho_f}{K}\sum_{q=1}^{K}\vec{e}_k^{T}\boldsymbol{\Delta}\boldsymbol{\Delta}^T\vec{e}_q + 1 = \frac{\rho_f}{K}\sum_{q=1}^{K}\vec{e}_k^{T}\boldsymbol{\Delta}\mathbf{E}\boldsymbol{\Delta}^T + 1.\end{aligned} \tag{16}$$

Using (2.2), it is shown that $\vec{e}_k^{T}\boldsymbol{\Delta}\mathbf{E} = [1, \cdots, 1]$. From this fact and (2.16), one can conclude (2.14). ■

After (2.14) is proved, we provide an explanation from [1] as to why the variance of the effective noise term is invariant of the PDP. The precoder in

(2.4) is a matched filter whose impulse response is a time reverse and complex-conjugated image of the Channel Impulse Response (CIR). Hence, $n'_k[i]$ is composed of terms which consist of all non-zero auto-correlation lags of the CIR for the k-th user (ISI term in (2.10)), as well as all cross-correlation lags between CIR of user k and the CIR of the remaining $(K-1)$ users (MUI term in (2.10)). The effective MUI in $y_k[i]$ from the symbols intended for the q-th user depends only upon the total power in all channel correlation lags between CIRs of user k and user q. Due to the same channel and information symbol statistics for all users, the effective MUI in $y_k[i]$ from each of the remaining $(K-1)$ users is identical, and is independent of the individual PDPs. This means the total power in cross-correlation lags depends only upon the total power in the CIR for each user, which is independent of k due to (2.2).

2.3.2 Achievable Rate

The useful signal term in (2.9) is proportional to the zero-lag auto-correlation of the CIR for the k-th user. We claim that this zero-lag auto-correlation is $O(M)$ since it is the maximum gain combining of the lags and is proportional to the combining all tags power, which is proportional to the total channel power gain from the M base station antennas to the user k. Therefore, it is $O(M)$. With this in mind and all the information we had from the noise and the channel PDP, we can say the average power of the desired signal in (2.9) is given by

$$S_k = \mathbb{E}_{s_k[i]}\left[\left|\sqrt{\frac{\rho_f}{MK}}\sum_{l=0}^{L-1}\mathbb{E}\left[\vec{v}_l^H[k]\vec{v}_l[k]\right]s_k[i]\right|^2\right] = \frac{M}{K}\rho_f. \tag{17}$$

Proof. We are going to derive (2.17) step by step. First we have

$$\begin{aligned} S_k &= \frac{\rho_f}{MK} \times \mathbb{E}_{s_k[i]}\left[\left| \sum_{l=0}^{L-1} \mathbb{E}\big[\vec{v}_l^H[k]\vec{v}_l[k]\big] s_k[i] \right|^2 \right] \\ &= \frac{\rho_f}{MK} \times \mathbb{E}_{s_k[i]}\left[\sum_{l'=0}^{L-1} s_k^H[i]\mathbb{E}\big[\vec{v}_{l'}^H[k]\vec{v}_{l'}[k]\big] \times \sum_{l=0}^{L-1} \mathbb{E}\big[\vec{v}_l^H[k]\vec{v}_l[k]\big] s_k[i] \right]. \end{aligned} \tag{18}$$

For now, let's focus on the first multiplier, which is

$$\sum_{l'=0}^{L-1} s_k^H[i]\mathbb{E}\big[\vec{v}_{l'}^H[k]\vec{v}_{l'}[k]\big] = \sum_{l'}^{L-1} s_k^H[i]\mathbb{E}\big[\vec{e}_k^T \mathbf{D}_{l'}^{1/2} \mathbf{H}_{l'}^H \mathbf{H}_{l'} \mathbf{D}_{l'}^{1/2} \vec{e}_k\big]. \tag{19}$$

Note here $M \gg K$, so the K singular values of $\mathbf{H}_l$ are all roughly equal to $\sqrt{M}$ (as it is stated in (2.6)) [1]. So we can rewrite the expectation as

$$\begin{aligned} S_k &= \frac{\rho_f}{MK} \times \mathbb{E}_{s_k[i]}\left[\left| \sum_{l=0}^{L-1} \mathbb{E}\big[\vec{v}_l^H[k]\vec{v}_l[k]\big] s_k[i] \right|^2 \right] \\ &= \frac{M}{K}\rho_f \times \mathbb{E}\left[\sum_{l'=0}^{L-1}\sum_{l=0}^{L-1} s_k^H[i]\mathbb{E}\big[\vec{e}_k^T \mathbf{D}_{l'} \vec{e}_k\big]\mathbb{E}\big[\vec{e}_k^T \mathbf{D}_{l} \vec{e}_k\big] s_k[i] \right] \\ &= \frac{M}{K}\rho_f \times \mathbb{E}\left[s_k^H[i]\Big(\sum_{l'=0}^{L-1} d_{l'}[k] \sum_{l=0}^{L-1} d_l[k]\Big) s_k[i] \right]. \end{aligned} \tag{20}$$

By using (2.2), we can compute the final value of (2.20) and it is equal to

$$S_k = \frac{M}{K}\rho_f \times \mathbb{E}\big[s_k^H[i] s_k[i]\big] = \frac{M}{K}\rho_f. \tag{21}$$

Note that (2.21) is equal to (2.17). ∎

Using the equations (2.11) and (2.17), we can compute the k-th user achievable rate

$$R_k = \log_2\left(1 + \frac{M\rho_f}{K\rho_f + K}\right). \tag{22}$$

The achievable sum-rate therefore given by

$$R_{sum}(\rho_f, M, K) = \sum_{k=1}^{K} R_k = K \times \log_2\left(1 + \frac{M\rho_f}{K\rho_f + K}\right). \qquad (23)$$

We consider that all K users have approximately the same rate, so in order to compute the sum-rate, we multiply single user rate that we computed before in (2.22) by the number of users (i.e., K).

2.4 Channel Capacity

Capacity of a Gaussian channel is always considered as the upper bound for the user's rate. The sum-capacity for a MIMO block channel is given by beamforming along the right singular vectors of the effective channel matrix. It transforms the channel into a set of parallel channels over which Gaussian symbols are communicated. The power allocation is given by the water-filling scheme [1].

2.4.1 Cooperative Capacity

For frequency-selective Gaussian broadcast channel (GBC) that we consider, we are going to set the cooperative upper bound. Basically, we will acquire this upper bound by reducing the multiple-user channel to a single-user MIMO channel which means we consider users to be cooperative. We also consider perfect CSI at both ends (transmitters and receivers). We assume that transmission occurs in time and with large blocks where we can say block size is much larger than L. To avoid any inter-block interference, we consider the last few transmitted vector of each block to be zeros. With all of these in mind, the general expression for the cooperative upper bound (capacity) is given by

$$C_{coop} = \log_2 \big(1 + \frac{S_k}{\mathrm{Var}(n_k[i])}\big), \tag{24}$$

where $n_k[i]$ is the simple additive white Gaussian noise of the channel.

2.4.2 Users Capacity

To calculate the cooperative capacity, we again use the property of independent and identically distributed $\mathcal{CN}(0,1)$ entries of $\mathbf{H}_l$, for which we can say $\mathbf{H}_l^H\mathbf{H}_l \approx M \times \mathbf{I}_K$ when $M \gg K$. So the power gain for each parallel channel is approximately M. With a uniform power allocation of ρ_f/K across the parallel channels and using (2.17) and (2.24), the cooperative upper bound on the ergodic sum-capacity of the frequency selective Gaussian broadcast channel is given by

$$C_{coop}(\rho_f, M, K) \approx K \log_2 \left(1 + \frac{M\rho_f}{K}\right). \tag{25}$$

2.5 Simulation Results

Simulations are based on all equations that we mentioned before. Also, the PDP is considered to be exponential with $L = 4$ and $d_l[k] = \frac{e^{-\theta_k l}}{\sum_{i=0}^{3} e^{-\theta_k i}}$, $l = \{0, \cdots, 3\}$, where $\theta_k = \frac{K-1}{5}$, $k = \{1, \cdots, K\}$. As it is mentioned before, the achievable sum-rate is invariant of the channel PDP. Hence, any other PDP which satisfies (2.2) can also be considered and yield the same results. In Figure 2.1 it can be seen that when $\rho_f \ll 1$, channel matched filter performance is near the upper bound which means the performance of the channel matched filter is almost optimal. As it can be seen in Figure 2.1, the sum-rate is plotted as a function of ρ_f for $M = 50$ base station antennas and $K = 10$ receiver users. The sum-rate performance of the channel matched filter is given both by the theoretical expression in (2.23) and via simulations. In a similar way, the cooperative sum-capacity upper bound is computed by (2.25) and via simulations. As ρ_f increases, all the interference terms that were discussed before dominate over the white noise term in (2.10) and the effective noise variance is equal to $\rho_f + 1 \approx \rho_f$. Because of that, when $\rho_f \to \infty$, the sum-rate of the channel matched filter saturates to the value $K \log_2 \left(1 + \frac{M}{K}\right)$ which to the regards of M and K here, is equal to 25.85 bits per channel use (bpcu). This means that the approximation to the sum-capacity upper bound is almost tight.

In Figure 2.2, for a fixed number of users and a fixed per user rate of 1 bpcu, the minimum transmit power required by the channel matched filter is plotted as a function of the number of antennas at the base station. The minimum transmit power required by the channel matched filter can be reduced roughly 3dB with every doubling in the number of antennas at the base station (for sufficiently large M [1]). Also, there is a typical scenario in Figure 2.2, where OFDM is used (in [1] it is used for comparison). We can show that by considering OFDM transmission with $M \gg K$, the per user ergodic information rate is given by

$$r \approx \frac{T_u}{T_u + T_{cp}} \log_2 \left(1 + \rho_f^{\mathrm{NEW}\frac{M}{K}}\right), \tag{26}$$

in which ρ_f^{NEW} denotes the total transmitted power for OFDM transmission. T_{cp} and T_u are OFDM transmission parameters which are the duration of the cyclic prefix and the duration of the useful signal, respectively. Note that in practice, modern wireless standards need $X > 1$ OFDM symbols per coherence time interval. Each OFDM symbol consists of N_u channel uses for data transmission and N_{cp} channel uses for cyclic prefix.

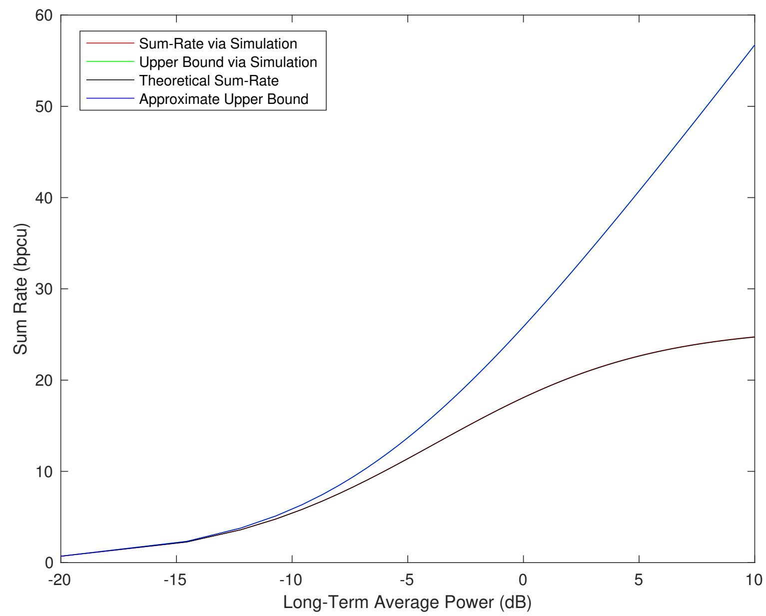

FIGURE 1: Sum rate of the matched filter and cooperative sum capacity upper bound vs ρ_f. Calculated for $M = 50$ base station antennas and $K = 10$ users.

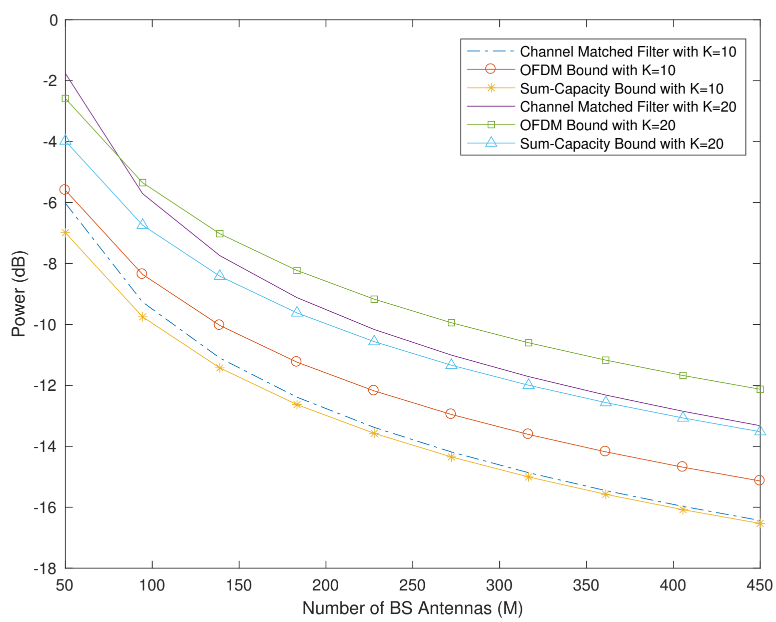

FIGURE 2: Minimum required transmit power to achieve a fixed per user information rate $r = 1$ bpcu as a function of the number of antennas at the base station.

2.6 Comparison

We now conclude our analysis in this chapter and also relate it to simulation results. As it is stated and shown in [1], when $\rho_f \ll 1$ and $M \gg K$, the channel matched filter performs in a near optimal fashion, meaning $R_{sum} \approx C_{coop}$. Analytically, when $\rho_f \ll 1$, the additive white Gaussian noise takes over the effective noise and dominates the interference terms in (2.10) and $\mathrm{Var}(n'_k[i]) \approx 1$. With this in mind, we can say $K\rho_f + K \approx K$ and therefore, sum-rate will be almost equal to sum-capacity. Also, this near optimality can be observed in Figure 2.1 where in the low-SNR region, the channel matched filter performs closely to the upper bound and it is clearly implying optimality. However, it can be observed in Figure 2.1 that as ρ_f increases and interference terms dominate the effective noise term in (2.10), the performance of the matched filter tends to saturate. Clearly one can say that if one uses the matched filter under interference-dominated circumstances, it is not going to perform well.

Using (2.23), the minimum transmit power that is required to achieve a fixed desired R_{sum} with respect to the number of users and antennas at the base station (i.e., K and M, respectively), can be written as

$$\rho_f(M, K) = \frac{K(2^{R_{sum}/K-1})}{M + K(2^{R_{sum}/K-1})}, \tag{27}$$

and $\lim_{M\to\infty} \frac{\rho_f(1,K)}{M\times\rho_f(M,K)} = \frac{1}{1+K(2^{R_{sum}/K-1})} > 0$. Hence, it follows that the matched filter achieves an $O(M)$ array gain power [1]. Therefore, for sufficiently large number of antennas at the base station, $\frac{\rho_f(M,K)}{\rho_f(1,K)} \propto \frac{1}{M}$ which means the total transmitted power can be reduced linearly by increasing M. This is supported by Figure 2.2. In this figure, for a fixed number of users and a fixed information rate per user (1 bpcu), the total minimum required power is plotted as a function of M. In Figure 2.2, it is also shown that for large number of antennas at the base station the total transmit power required by the matched filter is almost equal to the total transmit power required by a sum-capacity achieving scheme.

In OFDM transmission shown in Figure 2.2, we can say that to achieve an ergodic information rate per user for r bpcu, the minimum required transmitted power is given by

$$\rho_f^{NEW}(r) \approx \frac{K}{M}\big(2^{r(T_u+T_{cp})/T_u} - 1\big). \tag{28}$$

By using (2.24) we can say $\rho_f^{coop}(r) = \frac{K}{M}(2^r - 1)$. This is roughly equal to the required transmit power for the cooperative sum-capacity bound with rK bpcu. Under OFDM transmission, the additional transmitted power required for a fixed desired per user ergodic information rate, compared to a Gaussian broadcast channel sum-capacity achieving scheme is upper bounded by $\frac{\rho_f^{NEW}(r)}{\rho_f^{coop}(r)}$. Therefore, this additional transmit power (required under OFDM transmission) is given by $\frac{2^{r(1+T_{cp}/T_u)}-1}{2^r-1}$. Since it is larger than 1 and the total transmit power required by the channel matched filter is almost equal to the total transmit power of the sum-capacity achieving scheme, the channel matched filter under the circumstances of $\rho_f \ll 1$ and $M \gg K$ is more efficient compared to OFDM transmission. We would like to note in concluding that all of these results are for an independent channel.

Chapter 3

Dependent Channel

3.1 Introduction

We saw the channel matched filter performs nearly optimal when the fast and slow-varying components of the channel are independent from the locations, taps, and base station antennas. But the main question is what will happen to the channel matched filter results if the channel depends on one or more of those features. First, we will investigate what happens when there is dependency among base station antennas. Previously, we considered that $\mathbf{H}_l$ has independent and identically distributed complex normal entries. Now we will study the users' sum-rate in the situation that entries of $\mathbf{H}_l$ are not independent anymore. We will consider their dependence upon base station antennas. The implication of this is that the location of the antennas with respect to one another can affect the signal users receive. Antennas close to each other have stronger power to affect their nearby signals going out.

We do not expect improvement in the results of the channel with the presence of dependency. Actually, we expect that the result of the channel matched filter in the presence of considered dependency to degrade in terms of performance. When the channel has dependency on users, taps, or base station antennas, the transmitted signal will be changed significantly during communication through the channel. That is why we expect the channel matched filter to fail in the circumstances that the dependency exists.

We will show why the channel matched filter fails in the existence of dependency via analysis. We will discuss the difference between users' sum-rate now and before when the channel was independent. Then we will discuss results of the simulations and try to match them with analysis to explain the reasons of the degradation in the performance of the channel matched filter.

3.2 Base Station Dependency

We are interested in the signal that the m-th base station antenna is transmitting. Previously, we considered that base station antennas transmit independently of each other. But now the situation is different. We now consider that antennas at the base station affect each other. The best way to show the dependency is that if the specific antenna m_2 is closer to the antenna m_1 than the antenna m_3, it should have a stronger effect on the signal that the antenna m_1 is transmitting. This leads us to model the correlation among the antennas at the base station.

3.2.1 Antenna Correlation Model

Assume antenna m_i is in position i and antenna m_j is in position j. It is reasonable to expect, and is evidence in literature, that the effect of these antennas on one another should be related to $|i - j|$. We consider a basic correlation factor $0 < a < 1$ which shows the effects of antennas with respect to $|i - j|$ on each other where a is a real number. To show the effect of the distance in this modeling, we consider the correlation $a^{|i-j|}$ among base station antennas. This simple correlation models the effect of the distance. It will affect the channel realization matrix (i.e., $\mathbf{H}_l$).

We need to define the correlation matrix between base station antennas. By using the correlation between to antennas and expand it for all M antennas at the base station, we will have $\mathbf{A} \in \mathbb{C}^{M\times M}$ as the correlation matrix among base station antennas in which the elements are $[a]_{i,j} = a^{|i-j|}$. To demonstrate the effect of matrix $\mathbf{A}$ on the channel, we consider a new channel realization matrix $\tilde{\mathbf{H}}_l = \mathbf{A}^{1/2} \times \mathbf{H}_l$ in which $\mathbf{H}_l$ is the independent and identically distributed $\mathcal{CN}(0,1)$ channel realization without considering the correlation between base station antennas that we had before. With this in mind, we can use the new $\tilde{\mathbf{H}}_l$ to model the system with correlation between antennas.

3.2.2 System Model

We still want to use the channel matched filter as the precoder. This time we assume the transmitter knows the pattern of the correlation between antennas at the base station. So we design the channel matched filter based on the new channel realization. We can rewrite the received signal matrix as

$$\vec{y}[i] = \sum_{l=0}^{L-1} \mathbf{D}_l^{\frac{1}{2}} \tilde{\mathbf{H}}_l^H \vec{x}[i-l] + \vec{n}[i], \tag{29}$$

where $\vec{x}[i]$ is the transmitted signal vector and can be written as

$$\vec{x}[i] = \sqrt{\frac{\rho_f}{MK}} \sum_{l=0}^{L-1} \tilde{\mathbf{H}}_l \mathbf{D}_l^{\frac{1}{2}} \vec{s}[i+l]. \tag{30}$$

Note that (2.2) is still valid. Also, by defining $\tilde{\vec{v}}_l[k] = \tilde{\mathbf{H}}_l \mathbf{D}_l^{1/2} \vec{e}_k$, we can rewrite the received signal of the k-th user at time i as

$$y_k[i] = \sqrt{\frac{\rho_f}{MK}} \Bigg(\sum_{l=0}^{L-1} \mathbb{E}\big[\tilde{\vec{v}}_l^H[k]\tilde{\vec{v}}_l[k]\big] \Bigg) s_k[i] + n'_k[i], \tag{31}$$

in which the desired signal term and the effective noise term can be identified. Similarly, we can rewrite the effective noise term in (3.3) by using the new channel realization

$$\begin{aligned} n'_k[i] = &\sqrt{\frac{\rho_f}{MK}} \sum_{l=0}^{L-1} \Big(\tilde{\vec{v}}_l^H[k]\tilde{\vec{v}}_l[k] - \mathbb{E}[\tilde{\vec{v}}_l^H[k]\tilde{\vec{v}}_l[k]] \Big) s_k[i] \\ &+ \sqrt{\frac{\rho_f}{MK}} \sum_{\substack{a=1-L \\ a\neq 0}}^{L-1} \sum_{l=\max(a,0)}^{\min(L-1+a,L-1)} \tilde{\vec{v}}_l^H[k]\tilde{\vec{v}}_{l-a}[k] s_k[i-a] \\ &+ \sqrt{\frac{\rho_f}{MK}} \sum_{\substack{q=1 \\ q\neq k}}^{K} \sum_{a=1-L}^{L-1} \sum_{l=\max(a,0)}^{\min(L-1+a,L-1)} \tilde{\vec{v}}_l^H[k]\tilde{\vec{v}}_{l-a}[q] s_q[i-a] \\ &+ n_k[i]. \end{aligned} \tag{32}$$

where the first term is the additional interference (IF) term, the second term is the intersymbol interference (ISI) term, the third term is multiuser interference (MUI) term, and the last term is AWGN.

As the next step, we need to calculate the average of desired signal term over channel realization and symbols, similar to what we did for the independent case. Before doing that systematically, note that the structure we chose to model the dependency of the channel realization upon base station antennas does not change the signal power. This can be seen by intuition. Therefore, we can say the average power of the desired signal term in (3.3) can be shown as

$$S_k = \mathbb{E}_{s_k[i]} \left[\left| \sqrt{\frac{\rho_f}{MK}} \sum_{l=0}^{L-1} \mathbb{E}\big[\tilde{\vec{v}}_l^H[k]\tilde{\vec{v}}_l[k]\big] s_k[i] \right|^2 \right]. \tag{33}$$

In order to calculate (3.5) and also power of the effective noise (which we will see in the next section), we need the following lemma.

Lemma 1: Let $\vec{h} \triangleq [h_1, h_2, \cdots, h_M]^T$ be an M-dimensional random vector. If $\mathbb{E}[\vec{h}] = \vec{\mu}$ and $\mathrm{Cov}[\vec{h}] = \mathbf{\Theta}$, then

$$\mathbb{E}[\vec{h}^H \mathbf{A} \vec{h}] = \mathrm{tr}(\mathbf{A}\mathbf{\Theta}) + \vec{\mu}^H \mathbf{A} \vec{\mu}, \tag{34}$$

in which, $\mathbf{A}$ is a real and symmetric $M \times M$ matrix. Before calculating (3.5), we prove Lemma 1 as below.

Proof. We can write

$$\begin{aligned} \vec{h}^H \mathbf{A} \vec{h} &= (\vec{h} - \vec{\mu})^H \mathbf{A} \vec{h} + \vec{\mu}^H \mathbf{A} \vec{h} \\ &= (\vec{h} - \vec{\mu})^H \mathbf{A} (\vec{h} - \vec{\mu}) + \vec{\mu}^H \mathbf{A} \vec{h} + (\vec{h} - \vec{\mu})^H \mathbf{A} \vec{\mu}. \end{aligned} \tag{35}$$

If we take expectations over (3.7), we obtain

$$\mathbb{E}[\vec{h}^H \mathbf{A} \vec{h}] = \mathbb{E}\big[(\vec{h} - \vec{\mu})^H \mathbf{A} (\vec{h} - \vec{\mu})\big] + \vec{\mu}^H \mathbf{A} \vec{\mu}. \tag{36}$$

Let $x_j \triangleq h_j - \mu_j$. Therefore $\vec{x} = \vec{h} - \vec{\mu}$ and we obtain

$$\begin{aligned}
\mathbb{E}\big[(\vec{h}-\vec{\mu})^H \mathbf{A}(\vec{h}-\vec{\mu})\big] &= \mathbb{E}[\vec{x}^H \mathbf{A}\vec{x}] \\
&= \sum_{i=1}^{M}\sum_{j=1}^{M} \mathbb{E}[x_i A_{i,j} x_j] = \sum_{i=1}^{M}\sum_{j=1}^{M} A_{i,j}[\mathrm{Cov}(\vec{x})]_{i,j} \\
&= \sum_{i=1}^{M}\sum_{j=1}^{M} A_{i,j}[\mathrm{Cov}(\vec{h}-\vec{\mu})]_{i,j} = \sum_{i=1}^{M}\sum_{j=1}^{M} A_{i,j}[\mathrm{Cov}(\vec{h})]_{i,j} \\
&= \sum_{i=1}^{M}\sum_{j=1}^{M} A_{i,j}\Theta_{i,j} = \sum_{i=1}^{M}\sum_{j=1}^{M} A_{i,j}\Theta_{j,i} \\
&= \sum_{i=1}^{M}[\mathbf{A}\boldsymbol{\Theta}]_{i,i} = \mathrm{tr}(\mathbf{A}\boldsymbol{\Theta}),
\end{aligned} \tag{37}$$

as desired. ■

By using Lemma 1, it can be shown that (3.5) is equal to $\frac{M}{K}\rho_f$. Thus, we can claim the average power of the desired signal remains the same.

Proof. We explained by intuition why the average of the desired signal remains the same, even when there is dependency between base station antennas. Now we want to prove it systematically. Again we consider the average power of the desired signal as

$$\begin{aligned}
S_k &= \frac{\rho_f}{MK} \times \mathbb{E}_{s_k[i]}\left[\left|\sum_{l=0}^{L-1}\mathbb{E}\big[\tilde{\vec{v}}_l^H[k]\tilde{\vec{v}}_l[k]\big]s_k[i]\right|^2\right] \\
&= \frac{\rho_f}{MK} \times \mathbb{E}_{s_k[i]}\left[\sum_{l'=0}^{L-1} s_k^H[i]\mathbb{E}\big[\tilde{\vec{v}}_{l'}^H[k]\tilde{\vec{v}}_{l'}[k]\big] \times \sum_{l=0}^{L-1}\mathbb{E}\big[\tilde{\vec{v}}_l^H[k]\tilde{\vec{v}}_l[k]\big]s_k[i]\right].
\end{aligned} \tag{38}$$

In the same way, we can claim that the first multiplier can be written as

$$\sum_{l'=0}^{L-1} s_k^H[i]\mathbb{E}\big[\tilde{\vec{v}}_{l'}^H[k]\tilde{\vec{v}}_{l'}[k]\big] = \sum_{l'=0}^{L-1} s_k^H[i]\mathbb{E}\big[\vec{e}_k^T\mathbf{D}_{l'}^{1/2}\mathbf{H}_{l'}^H\mathbf{A}\mathbf{H}_{l'}\mathbf{D}_{l'}^{1/2}\vec{e}_k\big]. \tag{39}$$

Note that according to the structure that we chose for the base station antennas correlation, we claim when $M \to \infty$, then $\mathbf{H}^H\mathbf{A}\mathbf{H} \to M \times \mathbf{I}_K$. Let's focus on the term $\mathbb{E}[\tilde{\vec{v}}_l^H[k]\tilde{\vec{v}}_l[k]]$. If we expand this term, it will be

$$\mathbb{E}[\tilde{\vec{v}}_l^H[k]\tilde{\vec{v}}_l[k]] = \mathbb{E}\big[\vec{e}_k^T\mathbf{D}_l^{1/2}\mathbf{H}_l^H\mathbf{A}\mathbf{H}_l\mathbf{D}_l^{1/2}\vec{e}_k\big]. \tag{40}$$

Note that $\mathbf{D}_l^{1/2}\vec{e}_k = \sqrt{d_l[k]}\vec{e}_k$, we can rewrite (3.12) as

$$\mathbb{E}[\tilde{\vec{v}}_l^H[k]\tilde{\vec{v}}_l[k]] = \sqrt{d_l[k]}\mathbb{E}\big[\vec{h}_l'[k]\mathbf{A}\vec{h}_l[k]\big]\sqrt{d_l[k]}, \tag{41}$$

where $\vec{h}_l[k] \triangleq \mathbf{H}_l\vec{e}_k$. Note that $\mathbb{E}[\vec{h}_l[k]] = \mathbb{E}[\vec{h}_l'[k]] = 0$ and $\mathrm{Cov}[\vec{h}_l[k]] = \mathrm{Cov}[\vec{h}_l'[k]] = \mathbf{I}_K$. By using Lemma 1, we can say that the expectation is equal to $\mathrm{tr}(\mathbf{A})$ which is equal to M. So the average power of the desired signal remains the same. ■

Thus, the model of the dependency causes no change in the average desired signal power. By adding the correlation among antennas at the base station, the average power of our desired signal remains the same. Now we need to see its effect on the effective noise of the channel.

3.2.3 Effective Noise Power

By using the new channel realization, the dependency that we considered shows itself in the effective noise variance. By considering (3.4), the effective noise variance can be written as

$$\mathrm{Var}\big(n'_k[i]\big) = \frac{\mathrm{tr}(\mathbf{A}^2)}{M}\rho_f + 1, \tag{42}$$

where $\mathrm{tr}(\mathbf{A}^2)$ is actually the trace of squared of the correlation matrix between antennas at the base station.

Proof. By taking a look at (3.4), we will see that different terms in the equation are independent from each other. Therefore, we can write the variance of the effective noise as

$$\begin{aligned}
\mathrm{Var}(n'_k[i]) = \frac{\rho_f}{MK} \times \mathrm{Var}\Bigg[\sum_{l=0}^{L-1}\bigg(\tilde{\vec{v}}_l^H[k]\tilde{\vec{v}}_l[k] - \mathbb{E}[\tilde{\vec{v}}_l^H[k]\tilde{\vec{v}}_l[k]]\bigg)s_k[i]\Bigg] \\
+ \frac{\rho_f}{MK} \times \mathrm{Var}\Bigg[\sum_{\substack{a=1-L \\ a\neq 0}}^{L-1}\ \sum_{l=\max(a,0)}^{\min(L-1+a,L-1)} \tilde{\vec{v}}_l^H[k]\tilde{\vec{v}}_{l-a}[k]s_k[i-a]\Bigg] \\
+ \frac{\rho_f}{MK} \times \mathrm{Var}\Bigg[\sum_{\substack{q=1 \\ q\neq k}}^{K}\ \sum_{a=1-L}^{L-1}\ \sum_{l=\max(a,0)}^{\min(L-1+a,L-1)} \tilde{\vec{v}}_l^H[k]\tilde{\vec{v}}_{l-a}[q]s_q[i-a]\Bigg] \\
+ 1.
\end{aligned} \tag{43}$$

Note that the mean of IF, ISI, and MUI terms are zero and they are independent from one another. Also, note that $\mathrm{Var}(s_k[i]) = 1$ and the information symbols are independent from all other terms. By combining all summations in (3.4) we can rewrite (3.15) as

$$
\begin{aligned}
\mathrm{Var}(n'_k[i]) = {} & \frac{\rho_f}{MK}\sum_{q=1}^{K}\mathbb{E}_{s_k}\left[s_q^H[i]\sum_{l=0}^{L-1}\mathbb{E}_{H_l}\left[\left|\tilde{\vec{v}}_l^H[k]\tilde{\vec{v}}_l[q]\right|^2\right]s_q[i]\right] \\
& + \frac{\rho_f}{MK}\sum_{q=1}^{K}\sum_{a=1}^{L-1}\mathbb{E}_{s_k}\left[s_q^H[i-a]\sum_{l=a}^{L-1}\mathbb{E}_{H_l}\left[\left|\tilde{\vec{v}}_l^H[k]\tilde{\vec{v}}_{l-a}[q]\right|^2\right]s_q[i-a]\right] \\
& + \frac{\rho_f}{MK}\sum_{q=1}^{K}\sum_{a=1}^{L-1}\mathbb{E}_{s_k}\left[s_q^H[i+a]\sum_{l=a}^{L-1}\mathbb{E}_{H_l}\left[\left|\tilde{\vec{v}}_{l-a}^H[k]\tilde{\vec{v}}_l[q]\right|^2\right]s_q[i+a]\right] \\
& - \frac{\rho_f}{K}\sum_{l=0}^{L-1}\mathbb{E}\left[\left|s_k[i]\right|^2\right]\mathbb{E}\left[\tilde{\vec{v}}_l^H[k]\tilde{\vec{v}}_l[k]\right] + \frac{M\rho_f}{K} + 1.
\end{aligned}
\tag{44}
$$

Let's focus on term $\mathbb{E}\left[|\tilde{\vec{v}}_l^H[k]\tilde{\vec{v}}_{l-a}[q]|^2\right]$. We can expand this term as

$$
\mathbb{E}\left[|\tilde{\vec{v}}_l^H[k]\tilde{\vec{v}}_{l-a}[q]|^2\right] = \mathbb{E}\left[\tilde{\vec{v}}_{l'-a'}^H[q']\tilde{\vec{v}}_{l'}[k']\tilde{\vec{v}}_l^H[k]\tilde{\vec{v}}_{l-a}[q]\right]. \tag{45}
$$

If $q \neq q'$, all terms inside the expectations in (3.7) will be independent from each other and the final value of (3.17) will be zero. The result is the same for the cases that $k \neq k'$, $a \neq a'$, and $l \neq l'$. Thus, we can rewrite (3.17) as

$$
\mathbb{E}\left[|\tilde{\vec{v}}_l^H[k]\tilde{\vec{v}}_{l-a}[q]|^2\right] = \mathbb{E}\left[\tilde{\vec{v}}_{l-a}^H[q]\tilde{\vec{v}}_l[k]\tilde{\vec{v}}_l^H[k]\tilde{\vec{v}}_{l-a}[q]\right]. \tag{46}
$$

Note that in all the summations in (3.16), $a \neq 0$. By using $\mathbf{D}_l^{1/2}\vec{e}_k = \sqrt{d_l[k]}\vec{e}_k$ and $\vec{h}_l[k] = \mathbf{H}_l\vec{e}_k$, we have

$$
\begin{aligned}
& \mathbb{E}\left[|\tilde{\vec{v}}_l^H[k]\tilde{\vec{v}}_{l-a}[q]|^2\right] \\
& = d_{l-a}[q] \times \mathbb{E}\left[\vec{h}_{l-a}^H[q]\mathbf{A}\vec{h}_l[k]\vec{h}_l^H[k]\mathbf{A}\vec{h}_{l-a}[q]\right] \times d_l[k] \\
& = d_{l-a}[q] \times \mathbb{E}_{H_{(l-a)}}\left[\vec{h}_{l-a}^H[q]\mathbf{A} \times \mathbb{E}_{H_l}\left[\vec{h}_l[k]\vec{h}_l^H[k]\right] \times \mathbf{A}\vec{h}_{l-a}[q]\right] \times d_l[k].
\end{aligned}
\tag{47}
$$

By using Lemma 1, we can calculate (3.19). Note that $\mathbb{E}_{H_l}\big[\tilde{\vec{h}}_l[k]\tilde{\vec{h}}_l^H[k]\big] = 1$. Hence, we can rewrite (3.19) as

$$\begin{aligned}\mathbb{E}\big[|\tilde{\vec{v}}_l^H[k]\tilde{\vec{v}}_{l-a}[q]|^2\big] &= d_{l-a}[q] \times \mathbb{E}\big[\tilde{\vec{h}}_{l-a}^H[q]\mathbf{A}^2\tilde{\vec{h}}_{l-a}[q]\big] \times d_l[k] \\ &= d_{l-a}[q] \times \mathrm{tr}(\mathbf{A}^2) \times d_l[k].\end{aligned} \tag{48}$$

By using (3.20) in all the summations of (3.16) we obtain

$$\begin{aligned}\mathrm{Var}(n'_k[i]) = \frac{\mathrm{tr}(\mathbf{A}^2)\rho_f}{MK}\sum_{q=1}^{K}\sum_{a=1}^{L-1}\sum_{l=a}^{L-1}\big(d_{l-a}[q]d_l[k] + d_l[q]d_{l-a}[k]\big) \\ + \frac{\mathrm{tr}(\mathbf{A}^2)\rho_f}{MK}\sum_{q=1}^{K}\sum_{l=0}^{L-1} d_l[k]d_l[q] + 1.\end{aligned} \tag{49}$$

As it can be seen in (3.21), we have computed the value of the above summations in (2.15). By using (2.16) we have

$$\mathrm{Var}(n'_k[i]) = \frac{\mathrm{tr}(\mathbf{A}^2)}{M}\rho_f + 1 \tag{50}$$

■

Now that we know everything we need about the desired signal power and the effective noise of the system, we are able to develop an equation for the users' information rate. Note that (2.11) and (2.24) still hold for the users' sum-rate and cooperative channel sum-capacity.

3.3 Information Rates

By comparing (3.14) and (2.14), we notice the difference is in term $\frac{\mathrm{tr}(\mathbf{A}^2)}{M}$. Note that when $a = 0$, diagonal elements of $\mathbf{A}$ are equal to 1 and other elements are zero. Therefore, (3.14) and (2.14) are equal (i.e., $\mathbf{A}^2 = \mathbf{A} = \mathbf{I}_M$ and

$\mathrm{tr}(\mathbf{A}^2) = M$). When $a \neq 0$, diagonal elements of matrix **A** remain the same but other elements have non-zero values and since we chose the correlation such that $a > 0$, these values cannot be negative. This means that when $a \neq 0$, $\mathrm{tr}(\mathbf{A}^2) > M$ and therefore, $\frac{\mathrm{tr}(\mathbf{A}^2)}{M} > 1$. Thus, we can say that the power of the effective noise has been increased due to the channel dependency on the antennas at the base station. However, this dependency has no effect on the average power of the desired signal. This means that we expect noticeable loss in the users' information rate and therefore, users' sum-rate. Using (2.11), each user's information rate will be $R_k = \log_2\left(1 + \frac{M^2\rho_f}{K\mathrm{tr}(\mathbf{A}^2)\rho_f + KM}\right)$. Therefore, by considering the fact that each user's information rate is almost equal to the other users', we will have the sum-rate as

$$R_{sum}(\rho_f, M, K) = K\log_2\left(1 + \frac{M\rho_f}{K\frac{\mathrm{tr}(\mathbf{A}^2)}{M}\rho_f + K}\right). \tag{51}$$

Comparing this expression with (2.23), the denominator of the fraction inside the logarithm function increases compared to the independent case. Which means we face significant loss in the information rate. Note that we choose matrix **A** such that $[a_{ij}] = a^{|i-j|}$. So by increasing the parameter a, $\mathrm{tr}(\mathbf{A}^2)$ will increase exponentially. This means that if the correlation parameter is getting higher, the information rate (sum-rate) will decrease significantly.

3.3.1 Upper Bound

By using the cooperative capacity expression (2.24) and the fact that the average of the desired signal power remains the same as before (the independent case), we conclude that (2.25) for the sum-capacity is still valid. So in the case of dependency, the cooperative sum-capacity can be written as

$$C_{coop}(\rho_f, M, K) \approx K \log_2 \big(1 + \frac{M\rho_f}{K}\big) \tag{52}$$

This is not good, because the information rate of the users decreases, but the capacity is still the same. This means that when there is dependency between antennas at the base station, there is a huge gap (which depends on the correlation parameter) between users' sum-rate and the sum-capacity achieving scheme. Due to the correlation between the antennas, the performance of the channel matched filter significantly decreases. We show this loss of the performance of the channel matched filter through the simulations of the channel.

3.4 Simulation Results

In this part of simulations, we use the same PDP as before, exponential function with $L = 4$ and $d_l[k] = \frac{e^{-\theta_k l}}{\sum_{i=0}^{3} e^{-\theta_k i}}$, $l = \{0, \cdots, 3\}$, where $\theta_k = \frac{K-1}{5}$, $k = \{1, \cdots, K\}$. Note that any function that satisfies (2.2) can be used as the PDP of the channel (achievable sum-rate is invariant of the channel PDP). To keep the figures comparable with the independent case, we ran the simulations for a channel with $M = 50$ antennas at the base station and $K = 10$ users (i.e. the simulations characteristics of the independent channel).

In Figure 3.1, it can be seen that when the correlation parameter equals to 0.4, the performance of the channel matched filter under the influence of the correlation between the antennas at the base station is not that far from the independent channel matched filter. By increasing the correlation parameter from 0.4 to 0.7, the gap between performances of the channel matched filter of the dependent case and independent case is getting noticeable. As it can be seen in Figure 3.2, this gap is almost 10 bpcu when $\rho_f = 10$ dB.

In practice, a correlation parameter around 0.4 or 0.7 is not considered a high correlation factor. Setting the correlation parameter $a = 0.9$ or even higher between base station antennas is realistic in many cases. In Figure 3.3 and 3.4, the channel matched filter performance is shown when the correlation parameter is higher than or equal to 0.9. As it can be seen, with $a = 0.9$ or $a = 0.99$, the channel matched filter completely fails. Under these conditions, the channel matched filter saturates faster and fails to demonstrate an acceptable performance.

3.5 Conclusion

As the conclusion of this chapter, according to analytical and simulation results, it is shown that the channel matched filter is not a good choice in the case there exists a correlation between antennas at the base station. When the channel is independent (i.e., $a = 0$), the white Gaussian noise dominates the effective noise power. Thus, the channel matched filter is a good choice to send the information symbols in the shape of transmit signal through the channel. As ρ_f increases, the information rate starts to saturate until the interference terms take over the effective noise power. As the correlation grows, the process of saturation occurs sooner and faster. This correlation between antennas at the base station causes the interference terms to be stronger and more effective than AWGN.

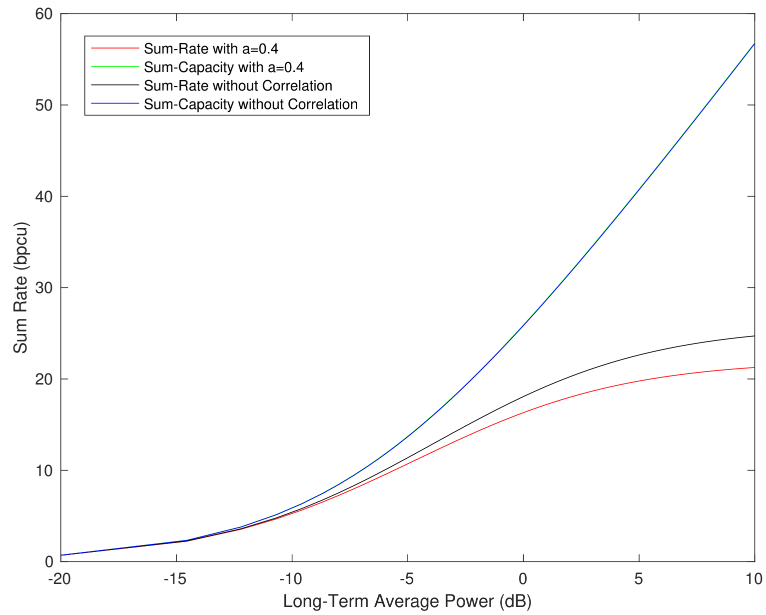

FIGURE 3: Sum rate and cooperative sum capacity upper bound as a function of ρ_f for a channel with correlation parameter $a = 0.4$.

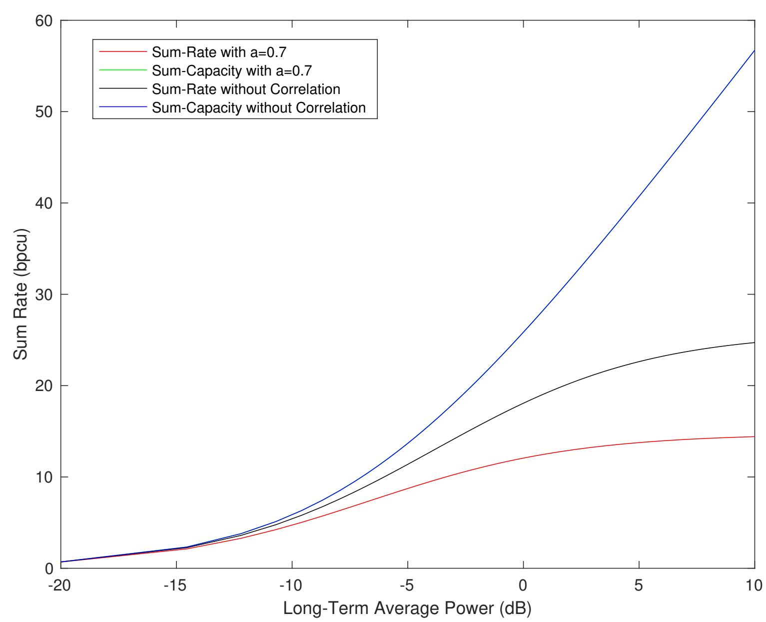

FIGURE 4: Information rate and capacity upper bound for a channel with correlation parameter $a = 0.7$.

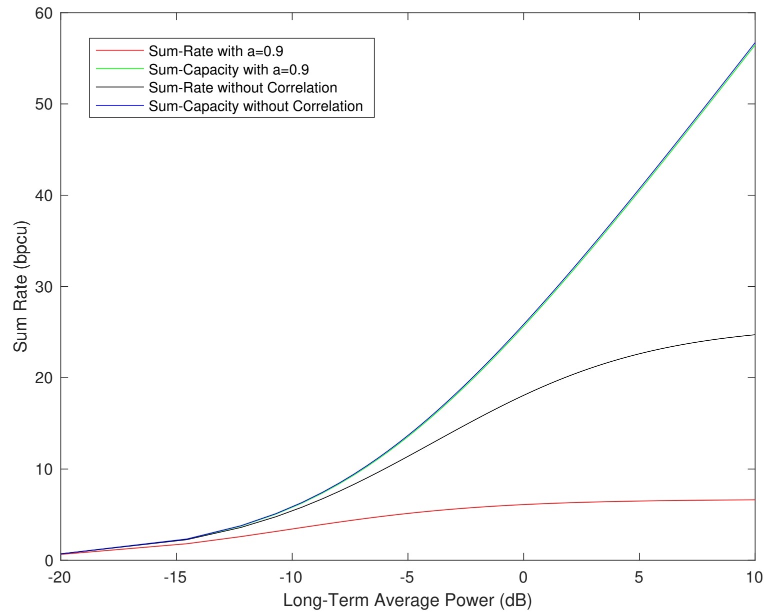

FIGURE 5: Users information rate and capacity for a channel with correlation parameter $a = 0.9$.

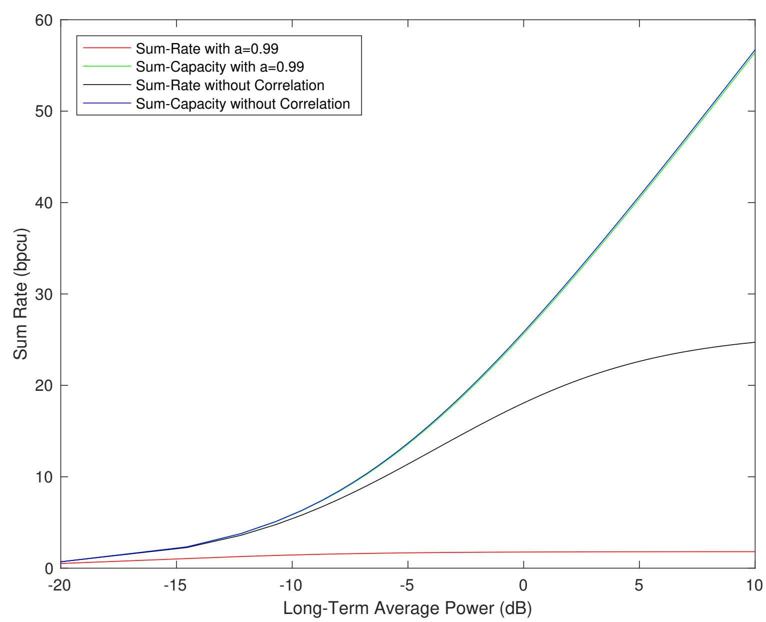

FIGURE 6: How information rate goes down with increasing the correlation parameter to $a = 0.99$

Chapter 4

Conventional Precoders

4.1 Introduction

As it is shown in Chapter 3, using the channel matched filter when the channel is independent from users, delay components, or transmitter antennas is nearly optimal. However, the channel dependency is shown to cause a failure in the channel matched filter performance. Transmission through a channel with dependency (i.e., a non-i.i.d. channel) needs more complicated preprocessing. There are a lot of precoders that have been considered to use for a non-i.i.d. channel [2]. We will consider three conventional precoders and replace the channel matched filter with them to improve the performance of the channel under the influence of interference between the channel's characteristics (i.e., base station antennas, users, or delay components). It is shown in [2] that using conventional precoders can increase power efficiency of the channel by decreasing Peak to Average Power Ratio (PAPR).

In this chapter, we will show the similarities and differences between single-carrier and OFDM transmission. We will see if using one of these two can actually improve the performance of the system on the channel we consider. Then we will introduce the conventional precoders and reevaluate the formulations that are developed in the previous chapters based on their characteristics. After obtaining the proper formulations, we will see the results of the simulations for an assumed i.i.d. channel (a channel without correlation) and compare them with the results of the channel matched filter. Also, we will run the simulations for a channel with a non-i.i.d. assumptions to see if these conventional precoders can improve the performance of the transmitter-receiver system in the non-i.i.d. case.

4.2 Single-Carrier vs. OFDM transmission

Before elaborating on the transmission techniques, it should be noted that block transmission with cyclic prefix has been considered in this thesis. A prefix, as a guard interval or as a delimiter between blocks, is presented in nearly all of the modern digital transmission methods. Although a prefix correlated with the symbols can be a waste of spectral resources, one can make this wasting of resources arbitrary small by choosing $N \gg L$.

As we discussed before, an achievable rate for user k in a channel (i.e., a downlink channel) is given by

$$R_k = \log_2(1 + \mathrm{SNR}_k), \tag{53}$$

where the signal-to-noise ratio (it can be seen as signal-to-interference-and-noise ratio to be exact) can be calculated using known channel's noise and inputs. For a non-linear amplification, there are two major consequences that can be seen in [2]. In-band distortion and signal clipping. Both consequences lead to a loss in power.

In terms of lower bound on the information rate (i.e., achievable data rate) in (4.1), which is tight when the channel hardens, single-carrier and OFDM transmission are nearly equivalent in massive MIMO [2]. Channels of all tones of OFDM transmission are in good status due to the channel hardening, therefore we can gain a little from the advantage of OFDM (i.e., the possibility of watefilling across frequencies). Thus, one can say if the same precoding scheme is used for all tones, the information rate showed in (4.1) is equal for single-carrier transmission and for OFDM [2].

In this thesis, as in [2], single-carrier transmission employs a recoding matrix defined in frequency domain. It is converted to time domain via an invert Fourier transform as will be specified in Section 4.3.2. It is beneficial to mention some of the differences between the two transmission methods. One of the main differences is that OFDM transmission requires the users to do a Fourier transform, while single-carrier transmission does not. On the other hand, OFDM transmission is less sensitive to synchronization errors in the sampling process since the symbol period of OFDM is longer than that of single-carrier transmission (i.e., NT compared to T) [2]. A small time synchronization error leads to a simple phase rotation in OFDM, while it leads to difficult intersymbol interference in single-carrier transmission. However, for small frequency synchronization errors, OFDM suffers from intersymbol interference and single-carrier transmission only experiences a simple phase rotation [2]. Also, OFDM transmission causes a delay of at least N symbols due to the block-by-block precoding and detection, while single-carrier transmission experiences smaller delay with implementation of short filters for frequency-selective channels [2].

4.3 Precoding Techniques

In wireless communication technologies the precoding scheme has a significant role. Note that by using precoding techniques, one can reduce PAPR and increase SNR at the receiver. This means that with the knowledge of the channel, the base station can precode the symbols in such a way that the signal's gain is large and the interference effect is small. We will focus on conventional precoders for the rest of this chapter.

4.3.1 OFDM Transmission

The precoder is defined typically in the frequency domain in OFDM transmission. Note that the time domain transmit signals are obtained from the inverse Fourier transform. The inverse Fourier transform of a vector $\vec{X}[f]$ in the frequency domain can be computed by

$$\vec{x}[i] = \sum_{f=0}^{N-1} e^{j2\pi i f/N} \vec{X}[f]. \tag{54}$$

We define $\mathbf{W}[f]$ as the precoding matrix for the frequency f. Since the precoding matrix depends only on the channel and not on the symbols, one can consider the precoding to be linear. Note that for the purpose of the formula, we can consider a constraint on the precoding matrix as

$$\mathbb{E}\left[|\mathbf{W}[f]|^2\right] = K, \forall f, \tag{55}$$

where K is the number of users.

4.3.2 Single-Carrier Transmission

In single-carrier transmission, the transmit signals are given by the cyclic convolution which is defined as

$$\vec{x}[i] = \sum_{l=0}^{N-1} \mathbf{W}[l]\vec{s}[i-l], \tag{56}$$

where the indices are taken modulo N. Note that the impulse response of the precoder is given in terms of its frequency domain counterpart and it can be written as

$$\mathbf{W}[l] = \sum_{f=0}^{N-1} e^{j2\pi fl/N}\mathbf{W}[f]. \tag{57}$$

4.3.3 Conventional Precoders

We introduce three different conventional precoders to be considered and studied for the channel. They will be given as functions of channel estimates matrix (i.e., $\mathbf{H}_l$) and its Fourier transform that can be computed by

$$\mathbf{H}_f = \sum_{l=0}^{L-1} e^{-j2\pi fl/L}\mathbf{H}_l. \tag{58}$$

(1) **Maximum-Ratio Precoding**: The maximum-ratio precoder aims at maximizing the gain and the received power of the desired signal. It is given by

$$\mathbf{W}_{MR}[f] = a_{MR}\mathbf{H}_f, \tag{59}$$

where a_{MR} is a power normalization factor.

While it maximizes the received power of the transmission, interference is still present in the received signal. In typical scenarios with favorable propagation, the maximum-ratio precoding suppresses this interference increasingly well with higher number of base station antennas (or increasing the transmitted signal's power) and in the limit of infinitely many antennas, the interference becomes negligible in comparison to the received power [2].

Note that in the case that we considered as a non-i.i.d. channel in the previous chapter, the interference has a significant effect on the received signal. Thus, the maximum-ratio precoding scheme might not be a perfect case to be considered for a non-i.i.d. channel. We will show the result of the simulations later in this chapter for this precoding scheme.

(2) **Zero-Forcing Precoding**: The zero-forcing precoder is given by

$$\mathbf{W}_{ZF}[f] = a_{ZF}\mathbf{H}_f \times \left(\mathbf{H}_f^H \mathbf{H}_f\right)^{-1}, \tag{60}$$

where a_{ZF} is again a normalization factor. The zero-forcing precoding scheme nulls the interference in the cost of lower gain in comparison with maximum-ratio precoding scheme [2].

(3) **Regularized Zero-Forcing Precoding**: The regularized zero-forcing precoding scheme maximizes the power of the desired signal compared to the power of the noise and interference at the receiver. In the limit of an infinite number of antennas, the optimal linear regularized zero-forcing precoder is given by

$$\mathbf{W}_{RZF}[f] = a_{RZF}\mathbf{H}_f \times \left(\mathbf{H}_f^H \mathbf{H}_f + \beta \mathbf{I}_K\right)^{-1}, \tag{61}$$

where a_{RZF} is a power normalization factor and $\beta \in \mathbb{R}^+$ is a system parameter which depends on the SNRs and the path losses of the users.

The interference and gain of the regularized zero-forcing precoding scheme depend on the parameter β. As it can be seen, the regularized zero-forcing precoder balances the interference suppression of zero-forcing and array gain of maximum-ratio precoding by changing the parameter β. How to find the optimal parameter β is described in [2].

It can be seen that when the transmit power is low compared to the noise variance at the receiver, then a large β is optimal and the interference and array gain are close to the ones of maximum-ratio precoding scheme. And when the transmit power relative the noise variance is high, a small β is optimal and the interference and array gain are close to the ones of zero-forcing precoding scheme.

4.4 System Model

Let the channel be an i.i.d. case without any dependency on its characteristics for now. We will study the non-i.i.d. case afterwards. Note that the received signal vector can be written as

$$\vec{y}[i] = \sum_{l=0}^{L-1} \mathbf{D}_l^{1/2} \mathbf{H}_l^H \vec{x}[i-l] + \vec{n}[i], \tag{62}$$

where we can extract the received signal at user k as

$$y_k[i] = \sum_{l=0}^{L-1} \vec{v}_l[k]^H \vec{x}[i-l] + n_k[i]. \tag{63}$$

By using the precoders that were discussed before, one can say that the signal that is sent into the channel can be computed using the precoders matrix. In order to consider all of the conventional precoding scheme in only one formula, let $\mathbf{W}[m]$ introduce the precoding matrix in a general case. Note that in the definition of the precoders, we already consider the normalization factor.

Therefore, the vector of the transmit signals is given by

$$\vec{x}[i] = \sum_{m=0}^{N-1} \mathbf{W}[m]\vec{s}[i-m]. \tag{64}$$

We also define $\vec{w}_k[m] \triangleq \mathbf{W}[m]\vec{e}_k$ as the vector of the precoding scheme related to user k at m-th sampled time. Note that $\vec{e}_k$ is a $K \times 1$ vector that all of its elements are zero except k-th element which is equal to 1.

By using (4.12) in (4.11), it can be seen that the received signal at user k is equal to

$$y_k[i] = \sum_{m=0}^{N-1}\sum_{l=0}^{L-1} \vec{v}_l^H[k]\mathbf{W}[m]\vec{s}[i-l-m] + n_k[i]. \tag{65}$$

Note that (4.12) represents the cyclic convolution and all the indices of equation defining the transmit signal are taken modulo N (where it can be seen that $N > L$). Therefore, we can rewrite (4.13) as

$$y_k[i] = \sum_{m=1-N}^{0}\sum_{l=0}^{L-1} \vec{v}_l^H[k]\mathbf{W}[m]\vec{s}[i-l-m] + n_k[i]. \tag{66}$$

By changing variable $m+l$ in (4.14) to a and considering the fact that $\vec{s}[i] = \sum_{q=1}^{K} \vec{e}_q s_q[i]$, we can rewrite (4.14) as the following

$$y_k[i] = \sum_{q=1}^{K}\sum_{a=1-N}^{L-1}\sum_{l=\max(0,a)}^{\min(N-1+a,L-1)} \vec{v}_l^H[k]\vec{w}_q[m]s_q[i-a] + n_k[i]. \tag{67}$$

Note that the desired signal is given by

$$S_k[i] = \sum_{l=0}^{L-1} \mathbb{E}\left[\vec{v}_l^H[k]\vec{w}_k[-l]\right]s_k[i]. \tag{68}$$

Using the equations of the desired and received signal, one can express the system model in terms of desired signal and effective noise of the channel.

Thus, we can rewrite (4.15) as

$$y_k[i] = \sum_{l=0}^{L-1} \mathbb{E}\big[\vec{v}_l^H[k]\vec{w}_k[-l]\big]\, s_k[i] + n'_k[i], \tag{69}$$

where n'_k represents the effective noise and can be written as

$$\begin{aligned} n'_k[i] &= \sum_{l=0}^{L-1} \left(\vec{v}_l^H[k]\vec{w}_k[-l] - \mathbb{E}\big[\vec{v}_l^H[k]\vec{w}_k[-l]\big]\right) s_k[i] \\ &+ \sum_{\substack{a=1-N \\ a\neq 0}}^{L-1} \sum_{l=\max(a,0)}^{\min(N-1+a,L-1)} \vec{v}_l^H[k]\vec{w}_k[a-l]s_k[i-a] \\ &+ \sum_{\substack{q=1 \\ q\neq k}}^{K} \sum_{a=1-N}^{L-1} \sum_{l=\max(a,0)}^{\min(N-1+a,L-1)} \vec{v}_l^H[k]\vec{w}_q[a-l]s_q[i-a] \\ &+ n_k[i], \end{aligned} \tag{70}$$

which includes IF, ISI, MUI, and AWGN terms, respectively. Note that the power normalization factor that we had in previous chapters is already considered in the definition of the precoder matrices.

In order to study the non-i.i.d. channel with dependency on the antennas at the base station, one can simply replace $\vec{v}_l[k]$ and $\vec{w}_k[l]$ with $\tilde{\vec{v}}_l[k]$ and $\tilde{\vec{w}}_k[l]$ respectively. Therefore, the effect of matrix **A**, which indicates the correlation between antennas at the base station and the channel dependency, will be considered inside of the precoding and the channel estimate vector.

With this system model, we can run the simulations to see if the conventional precoders are able to improve the final results.

4.5 Simulation Results

The performance of the conventional precoders is observed through numerical simulations for system with $M = 50$ antennas at the base station, $K = 10$ users (receiver antennas), and $L = 4$ taps. In order to compare the result of the conventional precoders and their performance on the channel, we also consider two cases of the channel, (i) an i.i.d. Gaussian channel with white noise, and (ii) a non-i.i.d. channel with correlation parameters $a \in \{0.4, 0.7, 0.9, 0.99\}$.

The results of the simulations for an i.i.d. channel (i.e., a channel with correlation parameter $a = 0$) using the conventional precoding schemes is shown in Figure 4.1. The top plot refers to the performance of the maximum-ratio precoders, the middle plot shows the result of the simulations for the zero-forcing precoder, and the bottom plot is the performance of the regularized zero-forcing precoding scheme.

Note that for the regularized zero-forcing precoder, we ran the simulations for the arbitrary parameter β, which in our simulations and the results showing in the figures of this chapter, $\beta = 2$.

As it can be seen in Figure 4.1, the performances of the precoders are not far from the optimal, which is using the channel matched filter. Also, for the channel with no correlation between antennas at the base station, all precoders perform equally well.

When it comes to a channel with correlation among antennas at the base station, one can see the difference between performances of the conventional precoders. In Figure 4.2, the information rate and the sum-capacity upper bound are plotted for maximum-ratio, zero-forcing, and regularized zero-forcing precoders for a channel with the correlation parameter $a = 0.4$. As it can be seen, zero-forcing and regularized zero-forcing precoders are almost the same

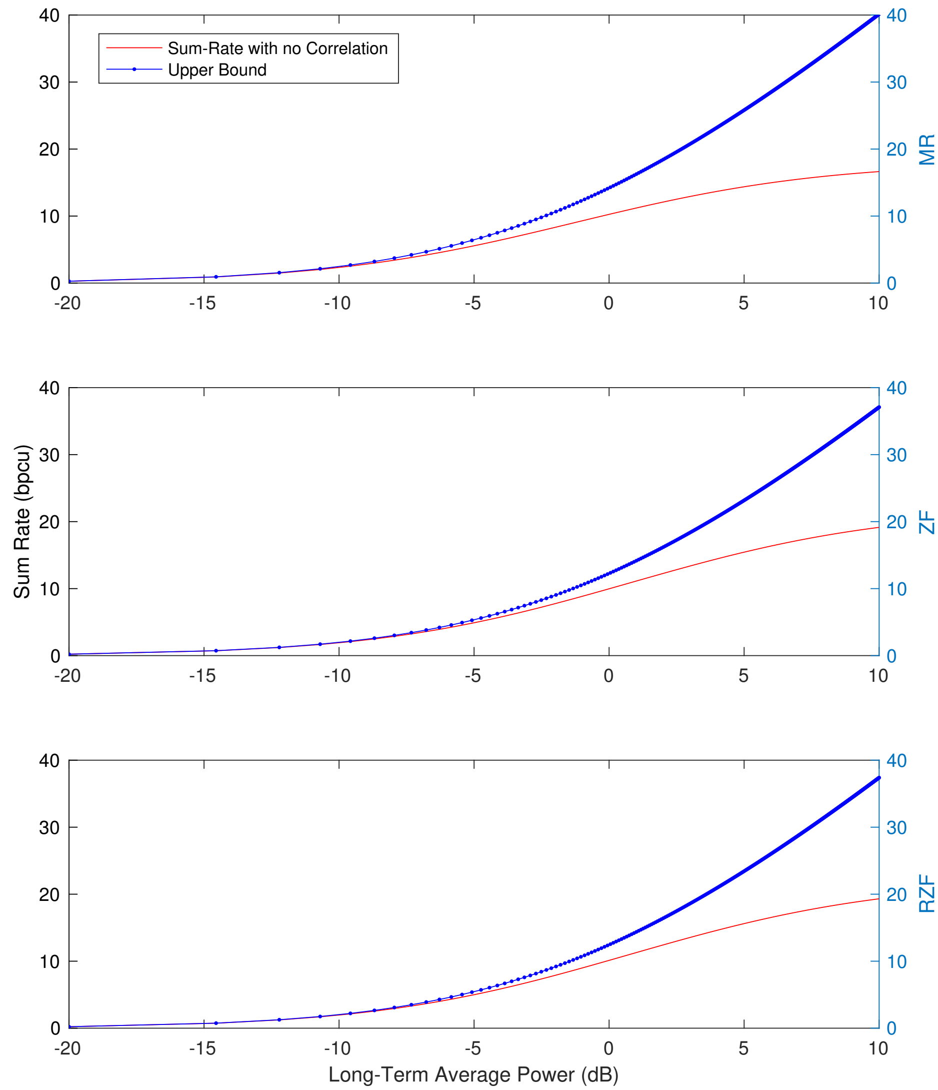

FIGURE 7: Users information rate and upper bound using the conventional precoders for an i.i.d. channel.

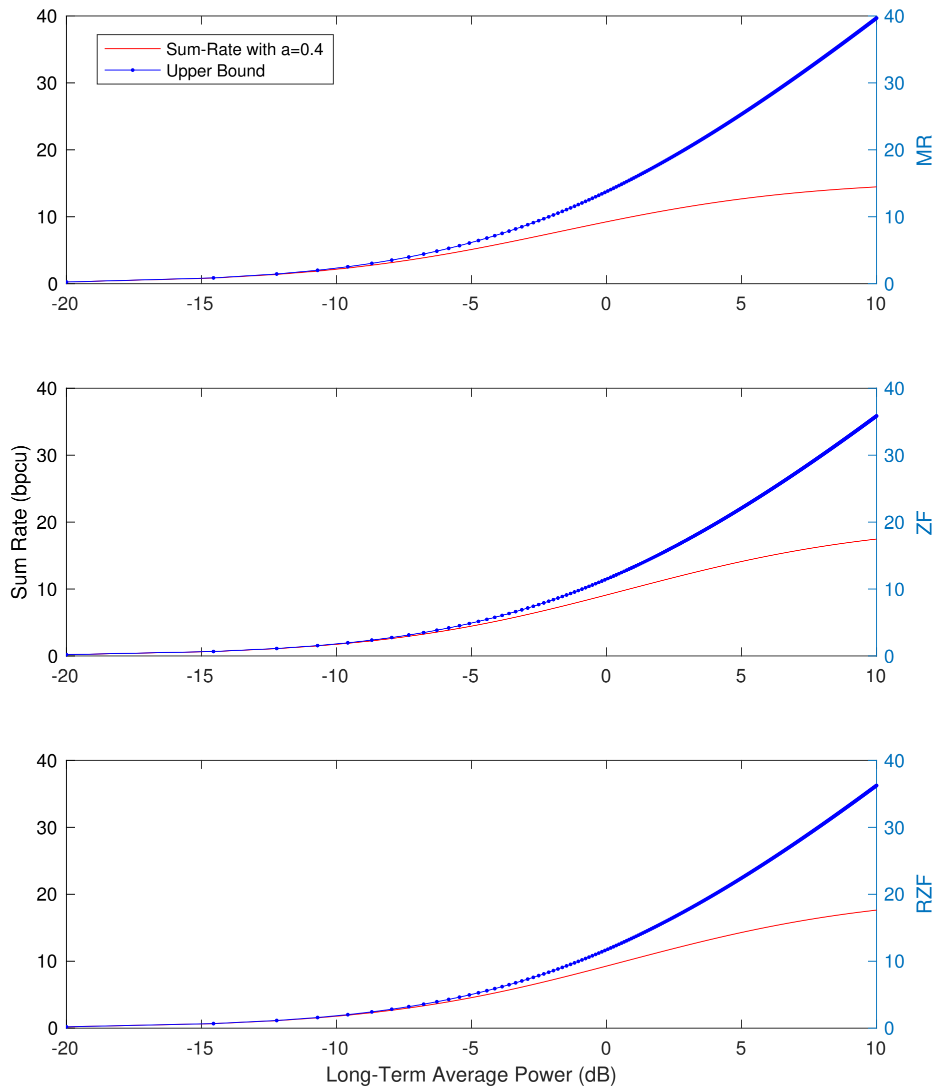

FIGURE 8: Sum rate and cooperative sum capacity upper bound as a function of transmit power using the conventional precoders for a channel with correlation parameter $a = 0.4$.

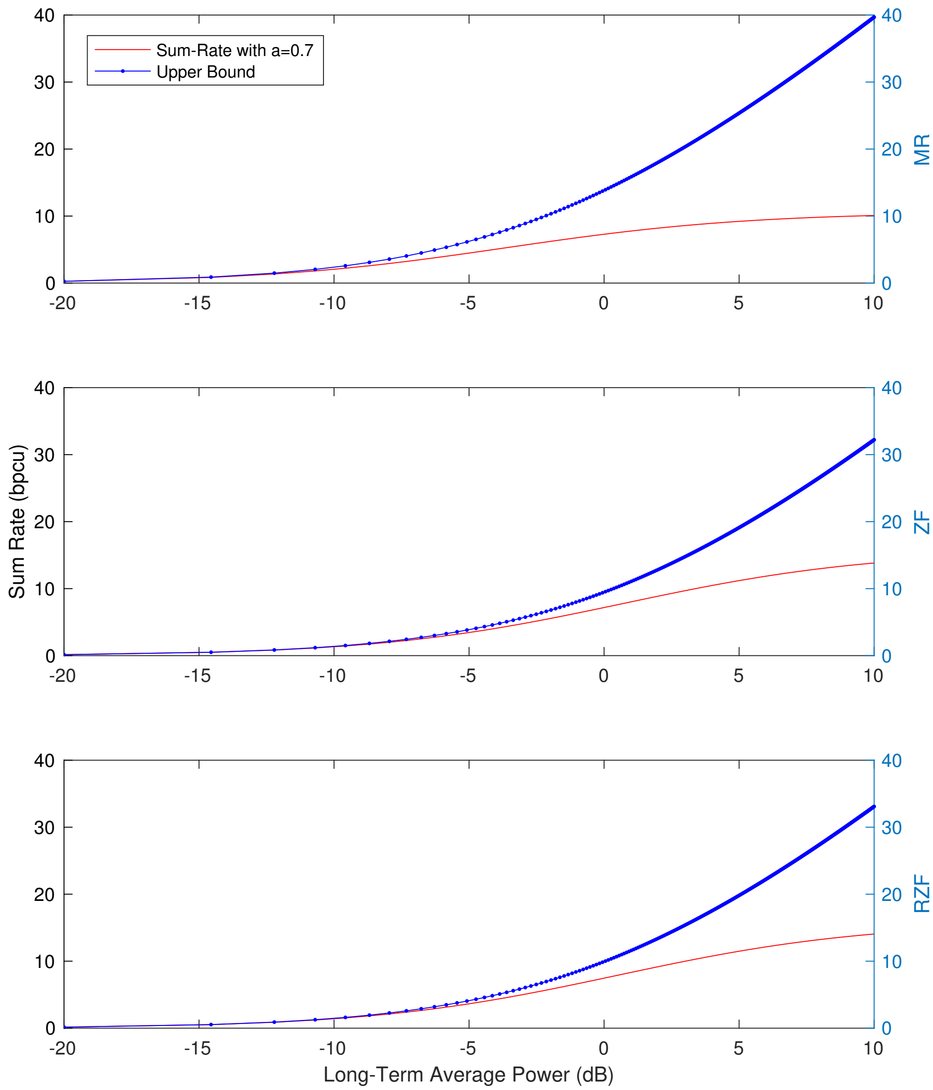

FIGURE 9: The performance of conventional precoders for a channel with correlation parameter $a = 0.7$.

in terms of the information rate, while maximum-ratio precoder has a gap in its information rate compared to the other precoders.

In Figure 4.3, the performance for a channel with the correlation parameter $a = 0.7$ is shown. As the correlation parameter goes higher, the difference between the maximum-ratio precoder and the other two stands out. While the zero-forcing and regularized zero-forcing precoders perform near their original performances (i.e., their performances in an i.i.d. channel), the maximum-ratio precoder begins to fail.

By increasing the correlation parameter to 0.9 and 0.99, shown in Figure 4.4 and Figure 4.5, the maximum-ratio precoder completely fails. However, the performances of the other two is still close to the upper bound of the channel. Note that since we use a dynamic method for normalizing the power, the upper bound changes by changing the correlation parameter, which causes a change in the channel estimate matrix and the transmit power.

4.6 Comparisons

From the figures provided in the previous section and the specific formulations related to the conventional precoders, one is able to compare these three precoders in terms of their performance and power consumption.

It can be seen that the maximum-ratio precoding scheme works well for low-rate requirements, but it is limited by interference to below a certain rate. Note that due to the distortion in SNR that scales with radiated power, all precoders have a vertical asymptote, above which the rate cannot be increased [2]. Therefore, one can say that the vertical asymptote of the maximum-ratio precoder is located at a lower rate than the asymptote of the zero-forcing and regularized zero-forcing precoders. Also, it can be noticed from figures in the

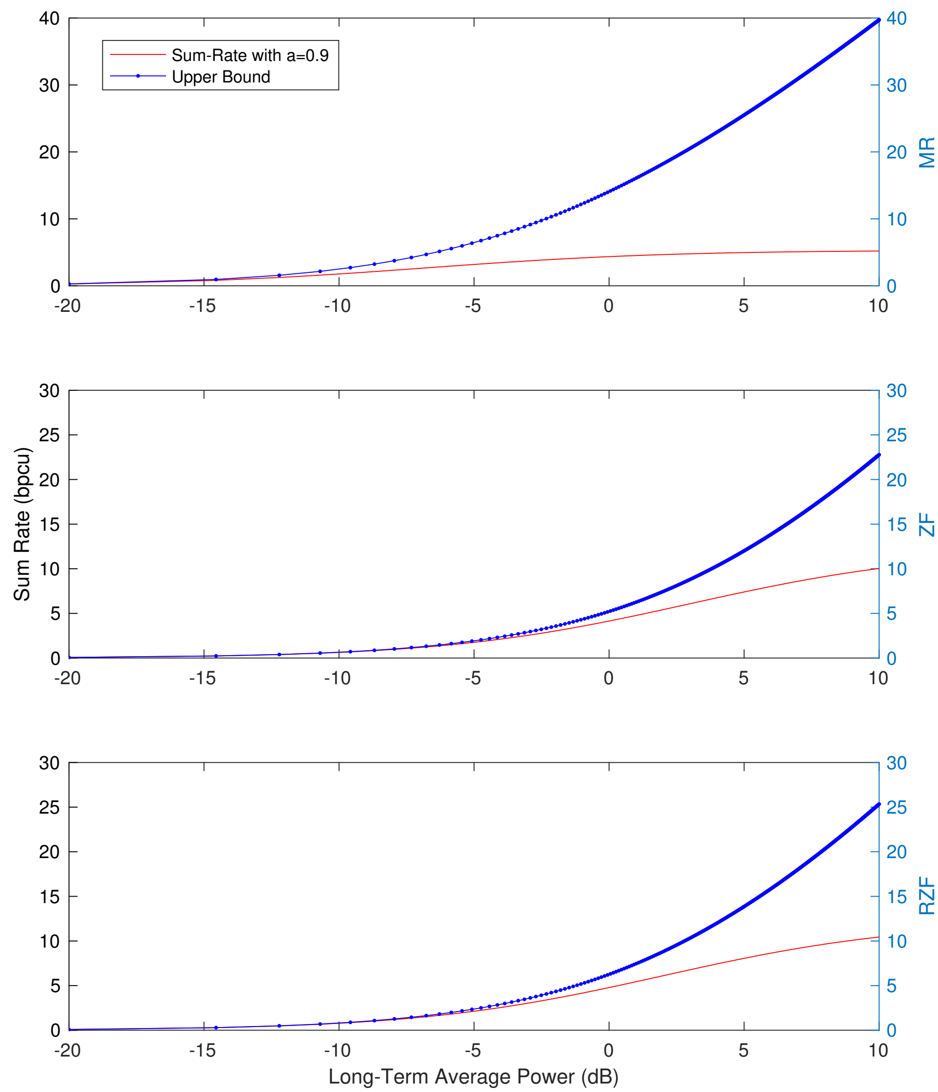

FIGURE 10: Sum rate and upper bound for a channel with correlation parameter $a = 0.9$.

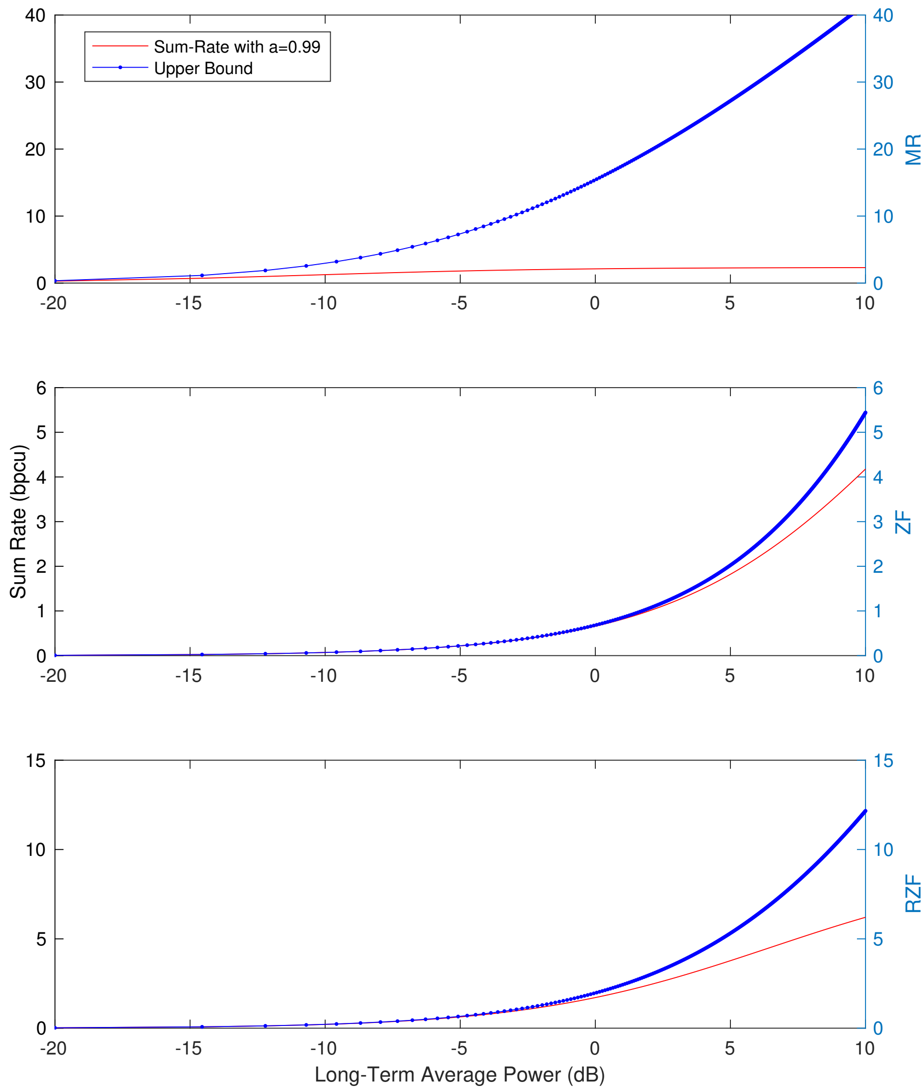

FIGURE 11: Information rate and upper bound for a channel with correlation parameter $a = 0.99$.

previous section that the maximum-ratio precoding scheme is more sensitive to the higher correlation parameter than the other two, which leads to the superiority of the zero-forcing and regularized zero-forcing precoders in the channels with high correlation amongst the antennas at the base station.

Furthermore, it can be shown that the zero-forcing and regularized zero-forcing perform equally well when the number of users is small besides performing well in channels with the high correlation parameter. Because of its ability to balance the resulting array gain and the amount of inter-user interference received by the users, the regularized zero-forcing has an advantage over zero-forcing precoder when it comes to a larger number of users.

Figure 4.6 shows a comparison between the regularized zero-forcing precoder and the channel matched filter when the base station consists of $M = 50$ antennas and provides information for $K = 10$ users (typical scenario we had before) in a channel without any correlation. As it can be seen, when the channel is correlation-free ($a = 0$), it is the channel matched filter that shows better performance and higher achievable data-rate and as SNR increases, the gap between information rate of these two increases.

Figure 4.7 shows the comparison between the channel matched filter and the regularized zero-forcing precoder when $M = 50$ antennas at the base station cover $K = 15$ users in the channel with no correlation. As it can be seen, the channel matched filter performs better in low-SNR cases, however, by increasing the power of the transmit signal (increasing SNR) the regularized zero-forcing precoding scheme starts to show a better performance even there is no correlation in the channel. This proves the statement that for larger number of users, precoders are expected to have superiority over the channel matched filter.

For a further comparison, the performances of the channel matched filter

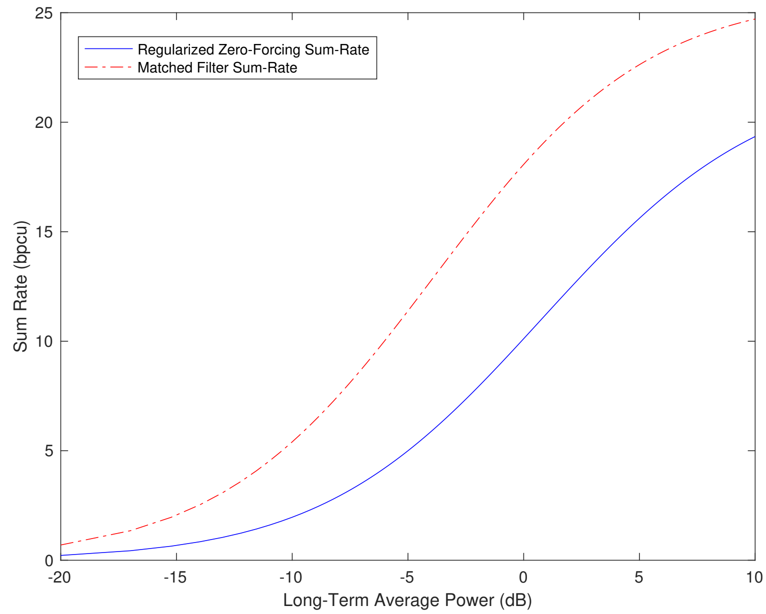

FIGURE 12: Comparison of the users information rate for $K = 10$ users in a channel with no correlation.

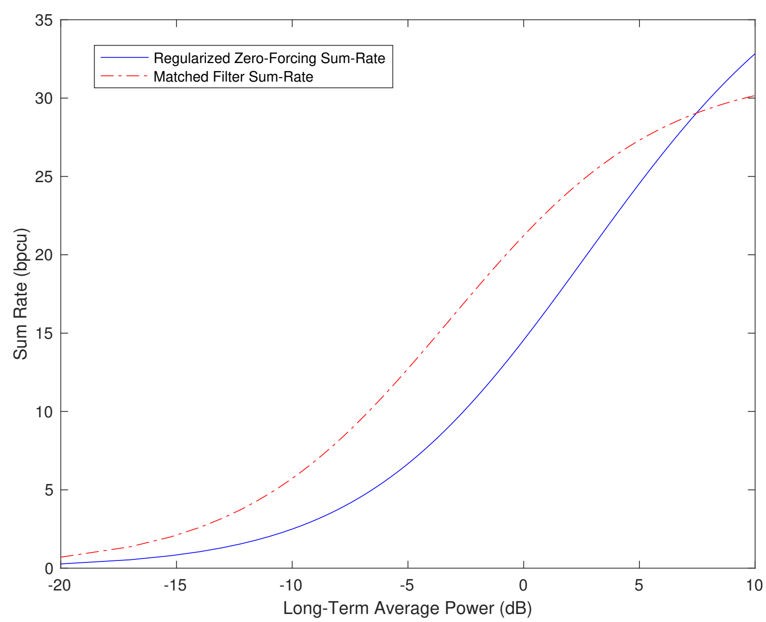

FIGURE 13: Comparison of the users information rate for $K = 15$ users in a channel with $a = 0$.

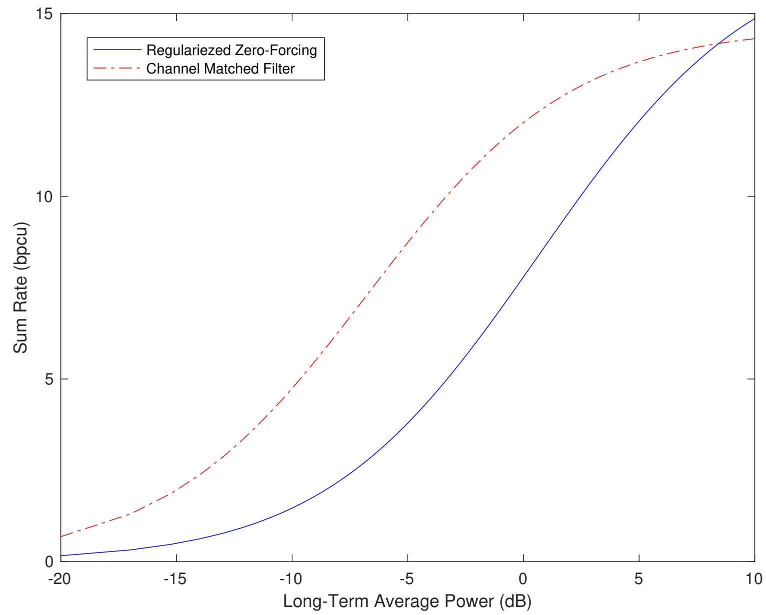

FIGURE 14: Performance of the channel matched filter and regularized zero-forcing for $K = 10$ users in a channel with $a = 0.7$.

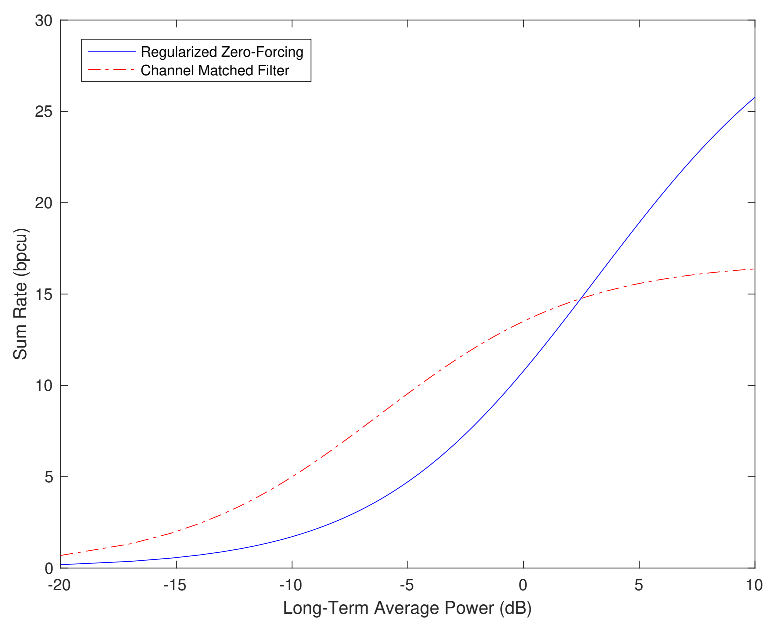

FIGURE 15: Achievable rate for $K = 15$ users in a channel with $a = 0.7$.

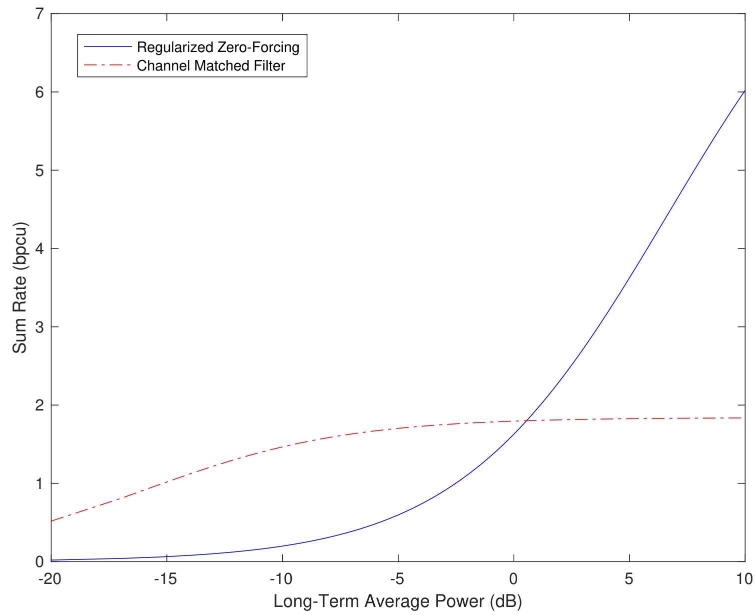

FIGURE 16: Performance of the channel matched filter and regularized zero-forcing for $K = 10$ users in a channel with $a = 0.99$.

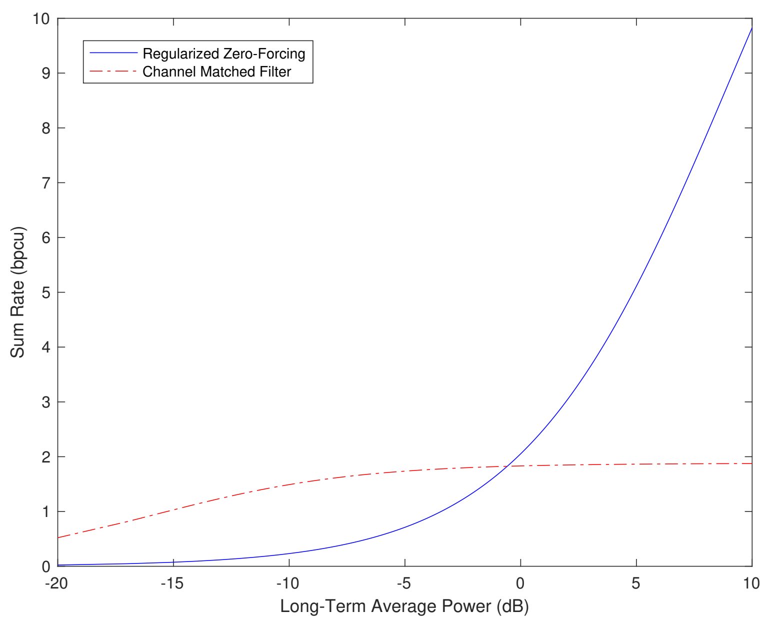

FIGURE 17: Achievable rate for $K = 15$ users in a channel with $a = 0.99$.

and the regularized zero-forcing precoder are shown in a channel with correlation. Figure 4.8 shows this comparison when the channel has correlation with parameter $a = 0.7$ and base station covers $K = 10$ users. Figure 4.9 shows comparison of the two in the same channel while base station antennas cover $K = 15$ users.

Also, Figure 4.10 and Figure 4.1 illustrate the performance of the two in the case that the channel correlation parameter increases to $a = 0.99$. Figure 4.10 shows this comparison when base station has $K = 10$ users to cover and Figure 4.11 shows the difference between the two when the number of users increases to $K = 15$. As it can be seen in both figures, the channel matched filter performs better when SNR is low. However, by increasing the input power, one can clearly see the difference between the performances of the two. A huge gap between the two curves (superiority of the regularized zero-forcing precoding scheme) is the corollary of increasing the SNR and the channel correlation parameter.

Chapter 5

Conclusion

5.1 Millimeter Waves and 5G

Wireless massive MIMO systems are able to serve a large number of users using multiuser precoding by a base station equipped with tens or hundreds of antennas. In modern wireless massive MIMO systems, an order of magnitude improvements is feasible in spectral and energy efficiency compared to classical multiuser MIMO. Hence, massive MIMO is expected to be a key component in the future wireless communications infrastructure [2].

As we discussed it before, the future wireless networks (5G) will be based, among others, on three main innovations with respect to the legacy of 4G systems. (i) the use of large scale antenna arrays (massive MIMO), (ii) the use of small-size cells in areas with a very large data request, and (iii) the use of carrier frequencies larger than 10GHz [4]. Since millimeter wave frequencies can successfully transmit very large data rates over short distances, they appear to be suited for providing wireless communications in a typical 5G scenario. Focusing on the use of carrier frequencies larger than 10GHz leads to propose millimeter wave frequencies as a strong candidate approach to achieve the spectral efficiency growth expected to be required by 5G wireless networks.

Although the use of millimeter wave signals for cellular communications has been neglected so far due to the higher atmospheric absorption that they suffer compared to the other frequency bands [4] and the larger values of free-space path-loss, the recent measurements in [2] and [3] suggest that millimeter waves attenuation during propagation in dense urban environments and short distances is slightly worse than attenuations in other bands.

Another feature of cellular communications at millimeter wave frequencies is that systems based on these frequencies are mainly noise-limited, which will simplify the implementation of interference management and resource scheduling policies [4].

5.2 System Model

One of the main questions about the use of millimeter wave bandwidths in the next generation of the cellular communication networks is about the type of modulation that will be used for these frequencies. There are several reasons that can be convincing about the use of single-carrier modulation for 5G networks at millimeter wave frequency ranges. First of all, the propagation attenuation of millimeter wave frequencies make them suitable for small cell, dense urban environment networks. In these type of cells, few users are assigned to any given base station, thus one can say the efficient frequency-multiplexing features of orthogonal frequency division multiplexing (OFDM) modulation may not be needed. Second, the large bandwidth for the next generation of the cellular networks seems to cause low OFDM symbol durations, which means with respect to small propagation delays, users may be multiplexed in the time domain as efficiently as in the frequency domain. Finally, massive antenna arrays can operate with millimeter wave frequencies to overcome propagation attenuation which makes digital beamforming unfeasible. This is the corollary of the huge required energy for digital-to-analog and reverse conversions. Thus, each user will have its own radio-frequency beamforming, which requires them to be separated in the time domain [4].

As we mentioned above, while it is not even certain that 5G systems will use OFDM modulation at classical cellular frequencies, there are sufficient reasons for us to say that single-carrier modulation on millimeter wave frequencies seem to be a valid candidate for the next generation of the wireless cellular networks. As a result, one can find the system model that we developed in Chapter 2 viable for the next generation of the wireless cellular networks.

5.3 Tap Correlation Model

In order to see other type of correlation in the channel, we develop circular-type dependency between delay components of the channel. Imagine that components which come from different taps in the channel are no longer independent and they are related to each other through a circular correlation matrix. We define this circular correlation such that the correlation among the delay components is defined by a rotation matrix. Since we want this correlation model to be simple and we are considering multiple taps for the channel, we only consider this rotation to be done in a plane (2-dimension) rather than the whole space of L-dimension.

We ran the simulations for the model mentioned above, in a channel with correlation among base station antennas and taps. A channel with $M = 50$ antennas at the base station, $K = 10$ users, and $L = 4$ taps has been considered and the results of the simulations for this channel are shown in Figure 5.1 through Figure 5.4. As it can be seen, the performance of the channel matched

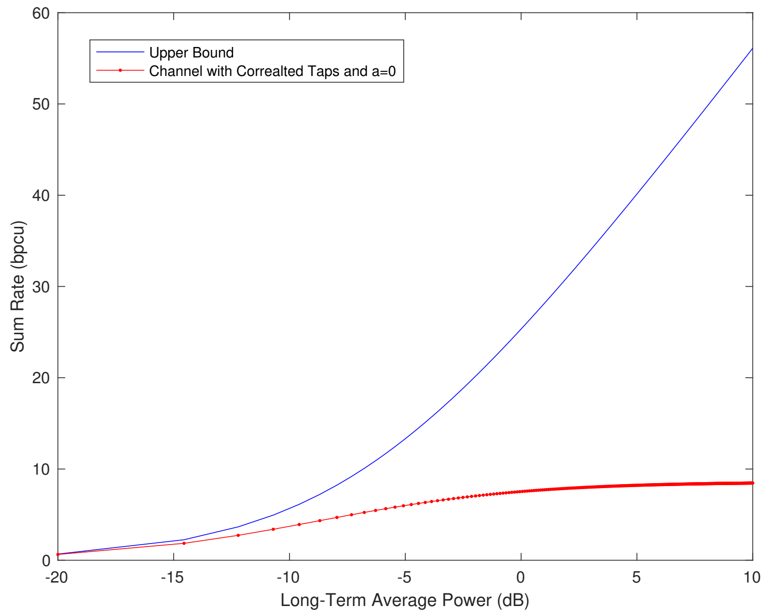

FIGURE 18: Performance of the channel matched filter in a channel with $L = 4$ correlated taps and $a = 0$.

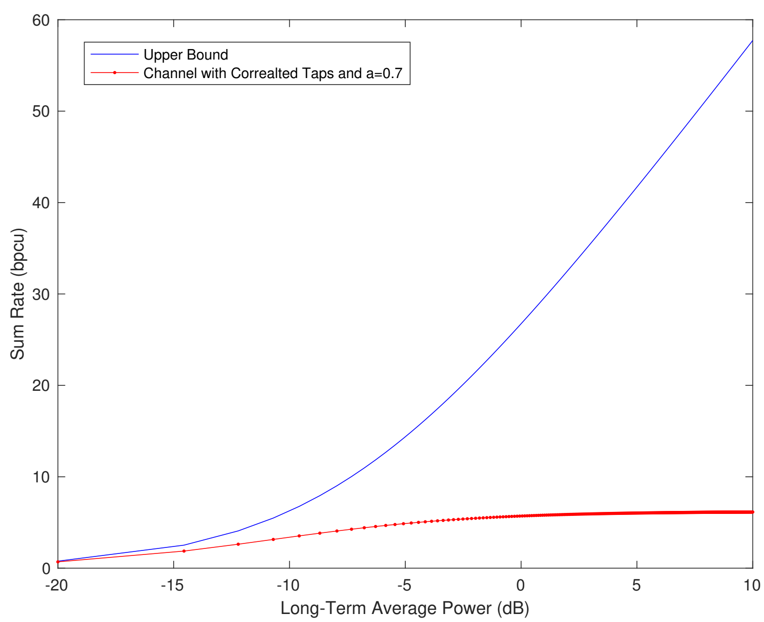

FIGURE 19: Information rate for the channel matched filter in a channel with $L = 4$ correlated taps and $a = 0.7$.

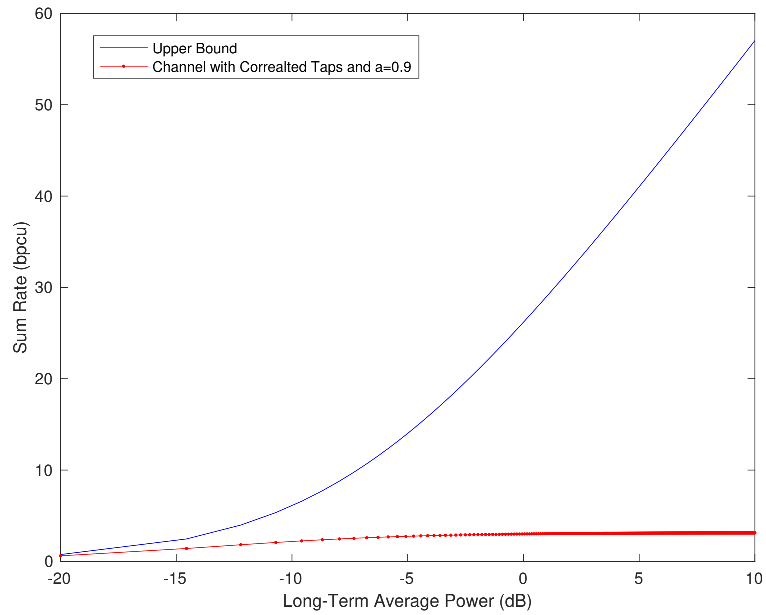

FIGURE 20: Performance of the channel matched filter in a channel with correlated taps and correlated antennas with $a = 0.9$.

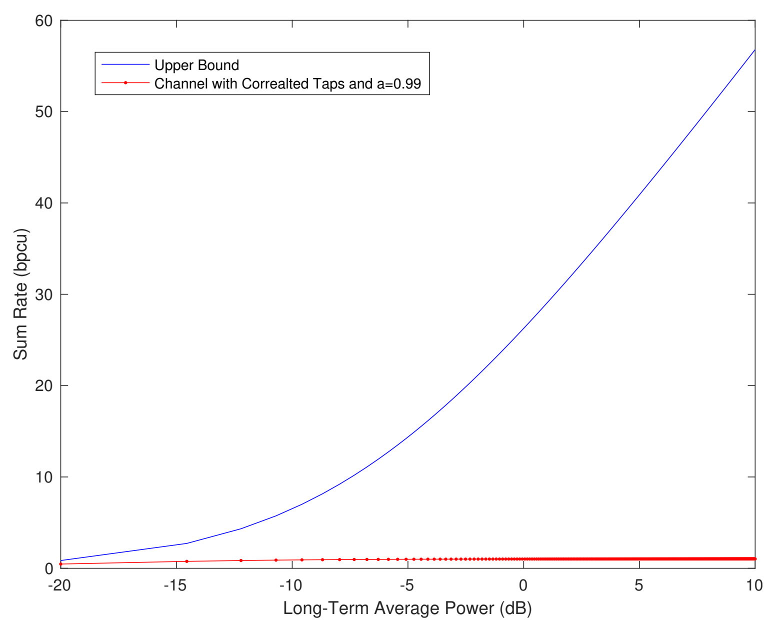

FIGURE 21: Information rate for the channel matched filter in a channel with correlated taps and $a = 0.99$.

filter when the taps are dependent to each other is not acceptable even in the case that antennas at the base station are independent. With increasing the correlation parameter among base station antennas, the information rate of the channel matched filter decreases dramatically.

We also ran the simulations on the same channel when the conventional precoders are used. The results of the simulation on the conventional precoders are shown in Figure 5.5 through Figure 5.8. Although the maximum-ratio precoder failed in the high correlation situation, the zero-forcing and the regularized zero-forcing showed better performance. As one can see, the gaps between the upper bound on the information rate in the channel and the achievable information rate by the zero-forcing and regularized zero-forcing precoders are not problematic. The zero-forcing and regularized zero-forcing precoder show a superior performance compared to the channel matched filter. However, the information rate of the zero-forcing precoder in a highly correlated environment is extremely low. Thus, we pick the regularized zero-forcing precoding scheme and compare it to the channel matched filter in terms of information rate. The results of the comparison are shown in Figure 5.9 through Figure 5.18.

As one can see, the results of the simulations on the channel with both taps and antennas correlations are similar to the ones with only correlation among antennas. Every pair of figures compares the results of the simulations for the channel matched filter and the regularized zero-forcing precoder in a channel with $L = 4$ correlated taps and correlation among antennas with the correlation parameters $a \in \{0, 0.4, 0.7, 0.9, 0.99\}$. Simulations are run for the channel when the base station has $M = 50$ antennas and cover $K \in \{10, 15\}$ users.

When the number of users is small and the environment has small correlations, the channel matched filter seems to have superiority in terms of performance and users' sum-rate. However, by increasing the number of users,

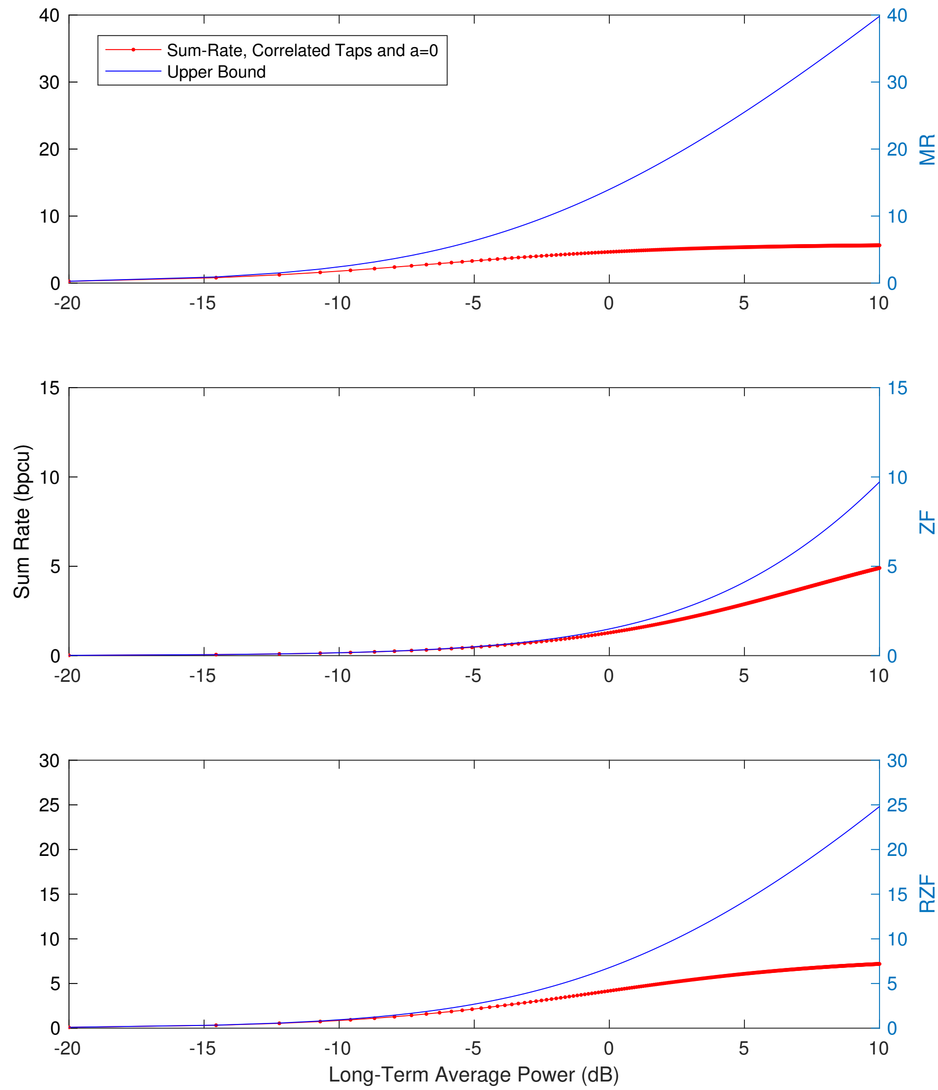

FIGURE 22: Information rate and upper bound for the conventional precoders in a channel with correlated taps.

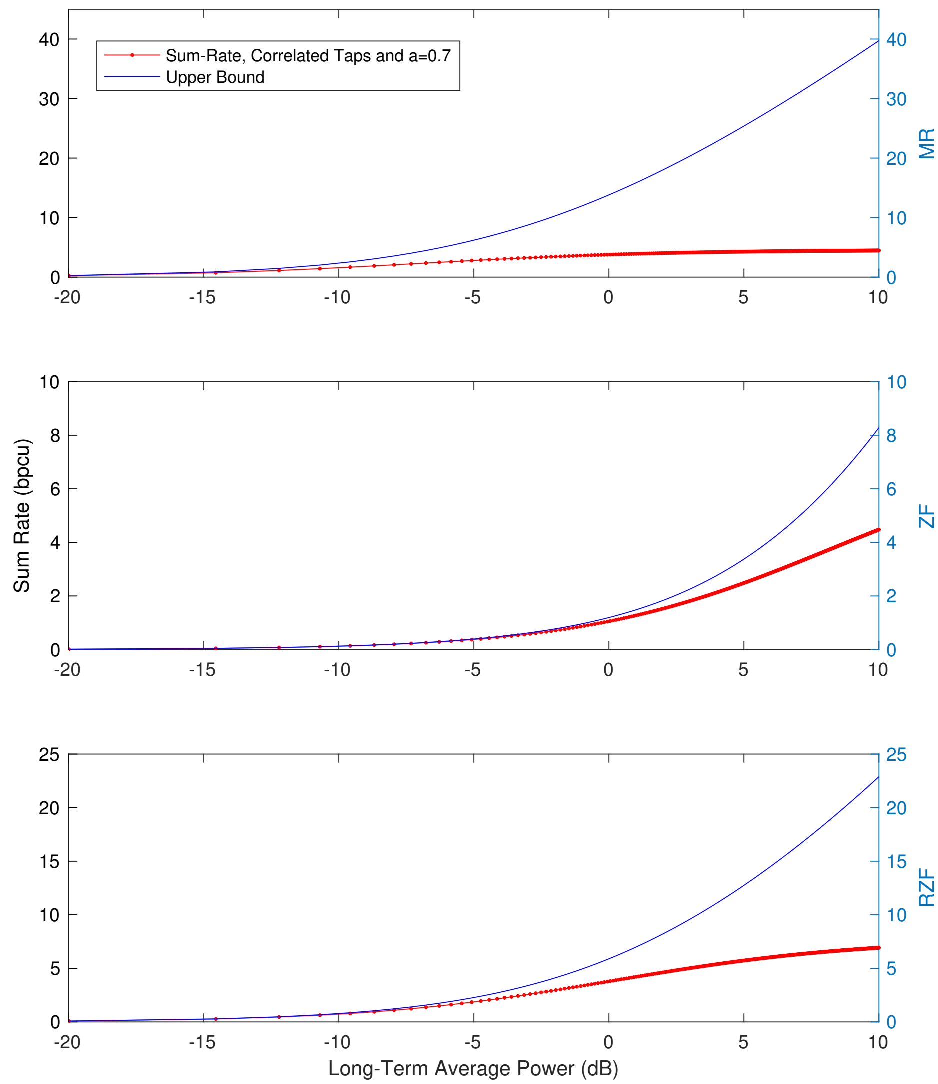

FIGURE 23: Achievable sum-rate for the conventional precoders in a channel with correlated taps and correlation parameter $a = 0.7$ among antennas.

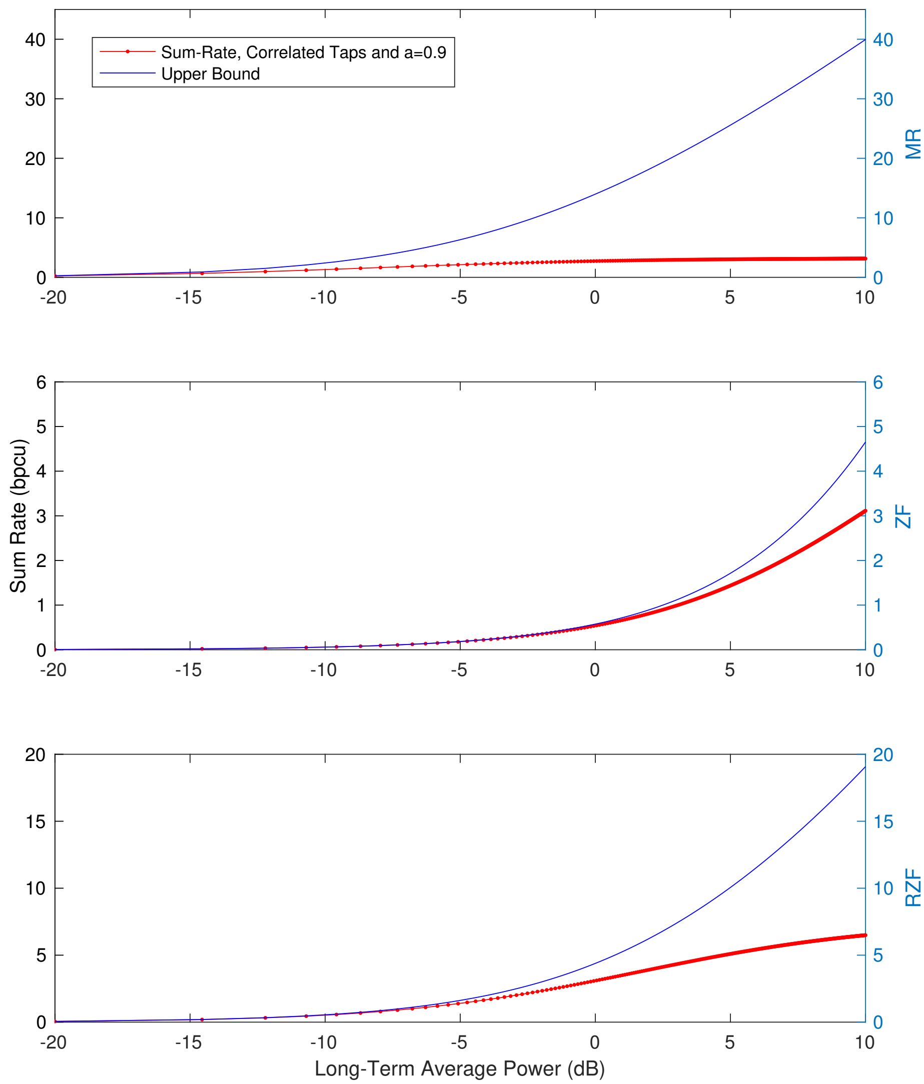

FIGURE 24: Upper bound and achievable rate of a channel with correlated taps and correlated antennas with correlation parameter $a = 0.9$ using the conventional precoders.

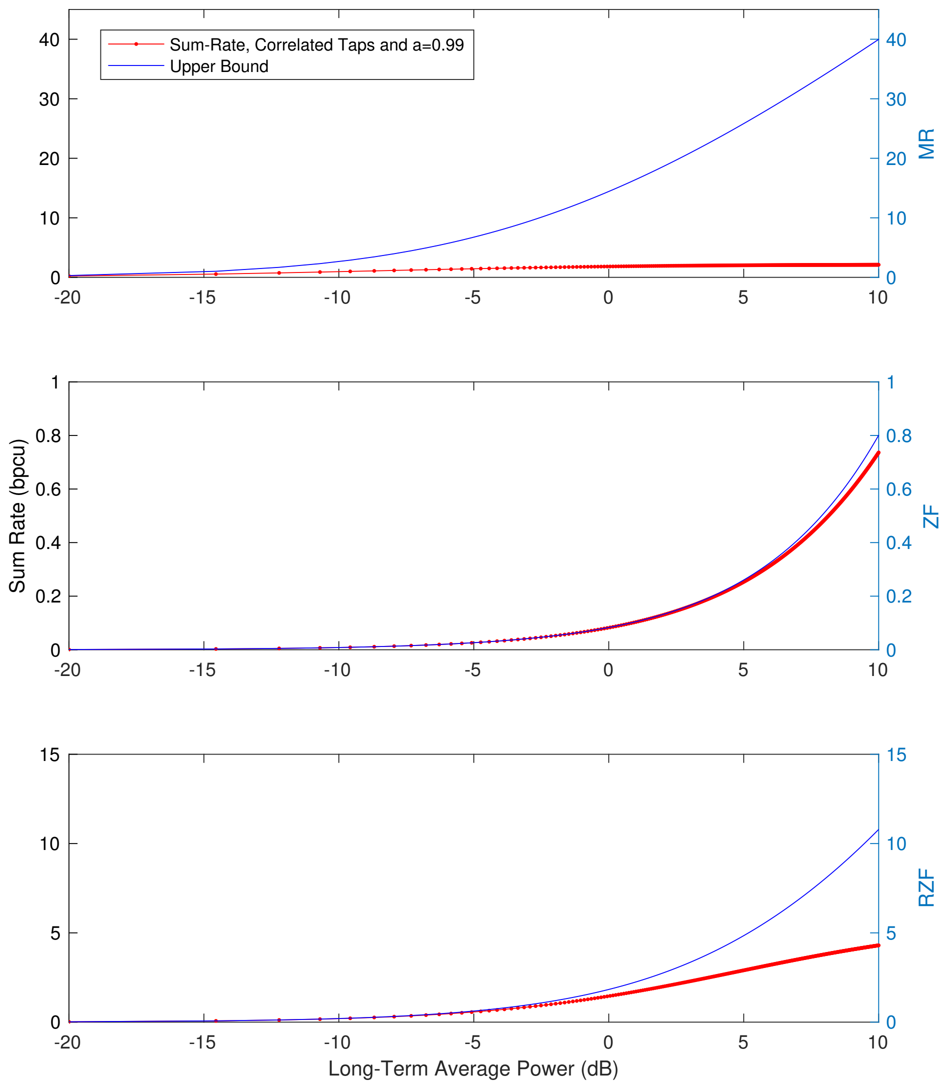

FIGURE 25: Information rate and upper bound for the conventional precoders in a channel with correlated taps and $a = 0.99$ among base station antennas.

or increasing the correlation parameter of the environment, one can see that the matched filter loses its superiority to the regularized zero-forcing precoder which performs near upper bound on the channel.

5.4 Equalization and Precoding

As a result of the simulations and all equations from previous chapters, one can say that sum-rate of a channel is highly dependent on the channel's situation. This means that without any types of correlations, the channel matched filter is expected to have optimal result and to perform near the upper bound of the channel. However, considering a correlation pattern among taps and/or antennas at the base station leads to a huge decrease in the achievable sum-rate for the users in the system. Thus, it can be expected to use a precoder (or equalizer) to compensate the loss of the users' sum-rate. In this work, we showed that in the highly correlated channels, using one of the mentioned conventional precoders can improve the performance of the channel in terms of users' sum-rate.

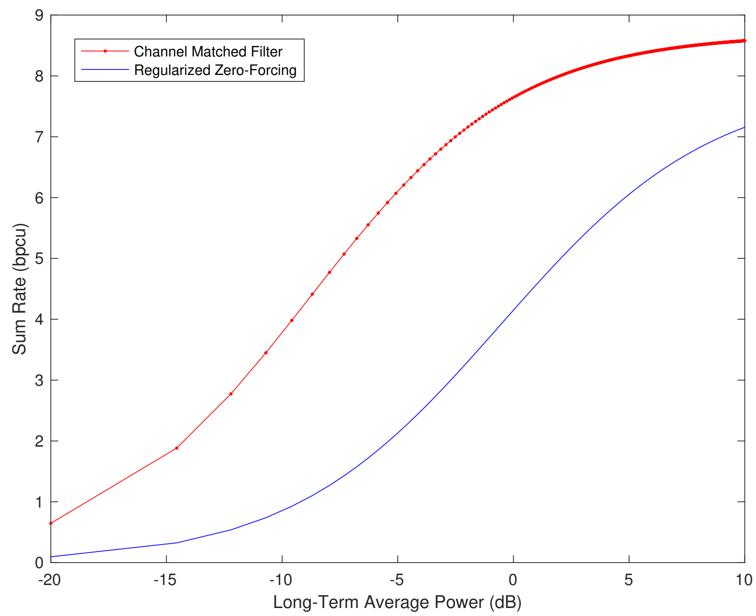

FIGURE 26: Performance of the channel matched filter and regularized zero-forcing for $K = 10$ users in a channel with correlated taps and $a = 0$.

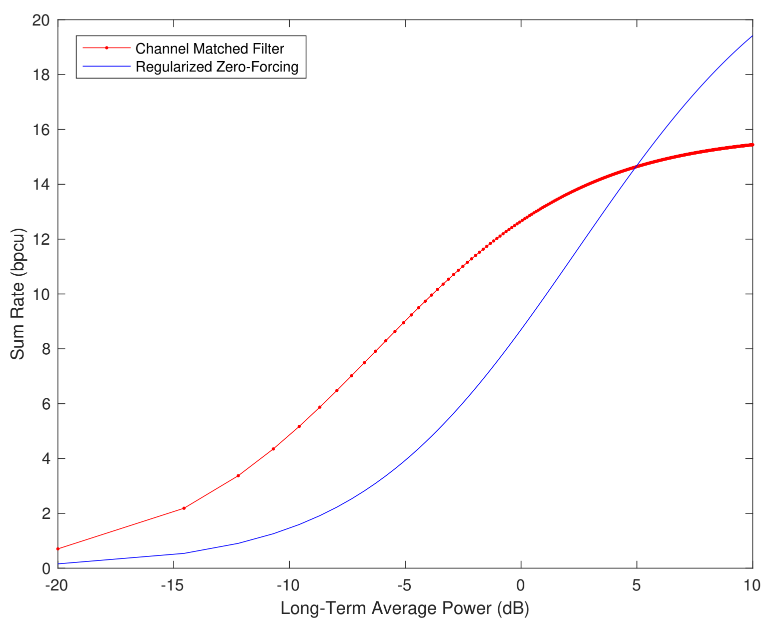

FIGURE 27: Achievable rate for $K = 15$ users in a channel with correlated taps and correlation parameter $a = 0$ among antennas.

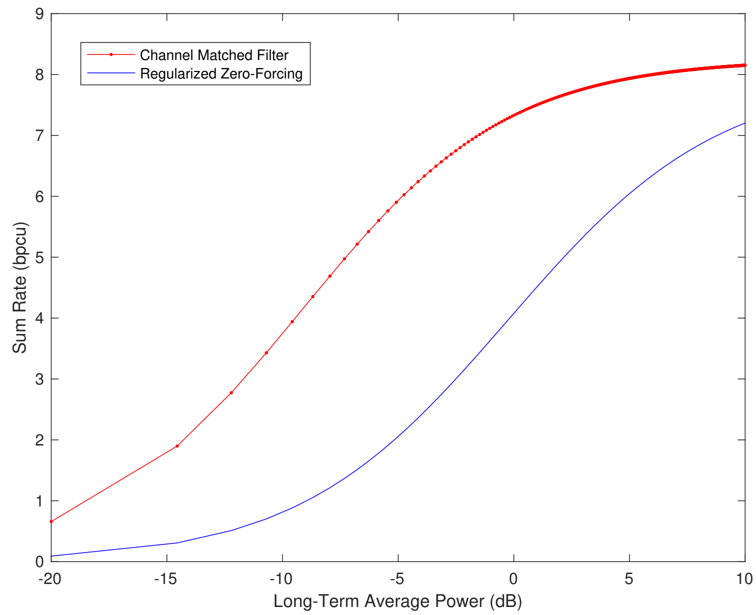

FIGURE 28: Information rate of the channel matched filter and regularized zero-forcing for $K = 10$ users in a channel with correlated taps and $a = 0.4$.

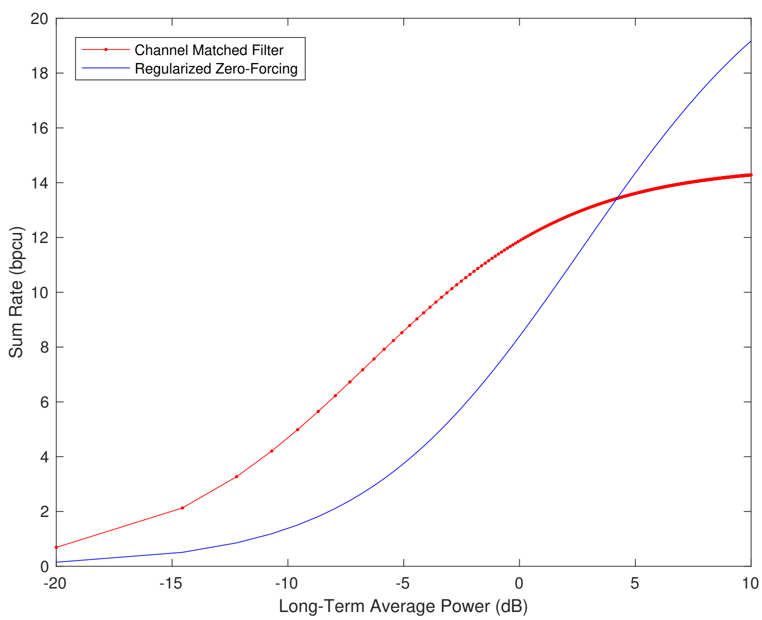

FIGURE 29: Achievable rate for $K = 15$ users in a channel with correlated taps and $a = 0.4$.

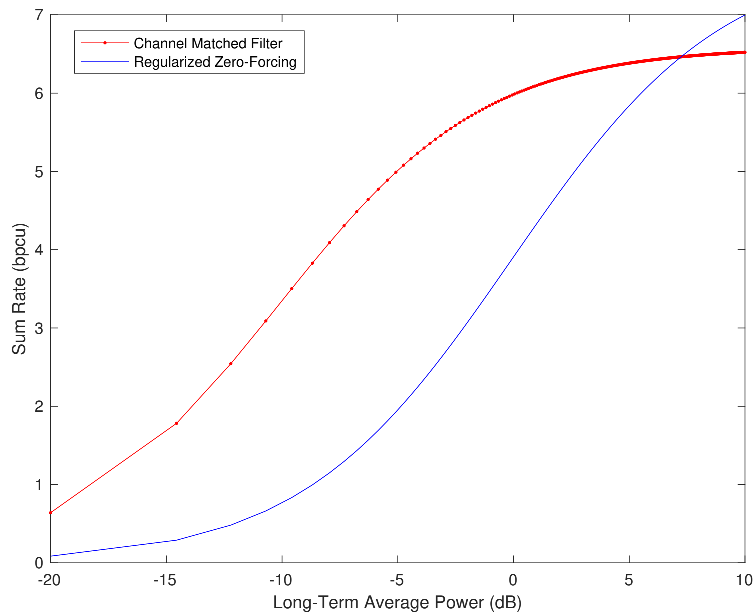

FIGURE 30: Performance of the channel matched filter and regularized zero-forcing for $K = 10$ users in a correlated-tap channel with $a = 0.99$.

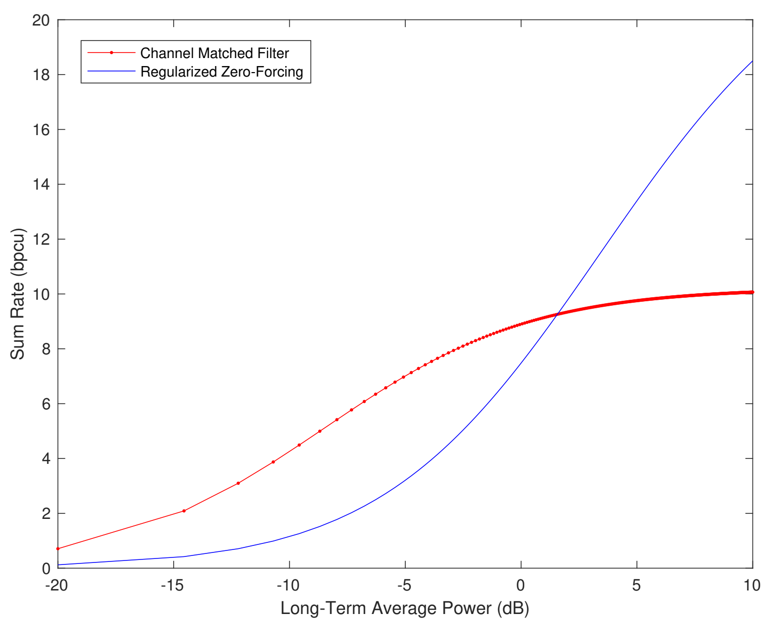

FIGURE 31: Users' sum-rate for a channel with correlation among taps and antennas with $a = 0.7$ correlation parameter and $K = 0.15$ users.

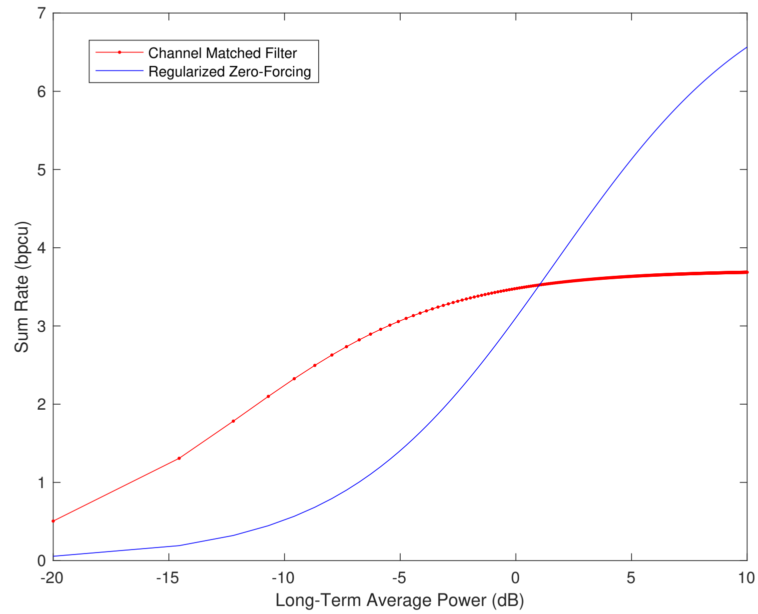

FIGURE 32: Performance of the channel matched filter and regularized zero-forcing for $K = 10$ users in a correlated-tap channel with $a = 0.99$.

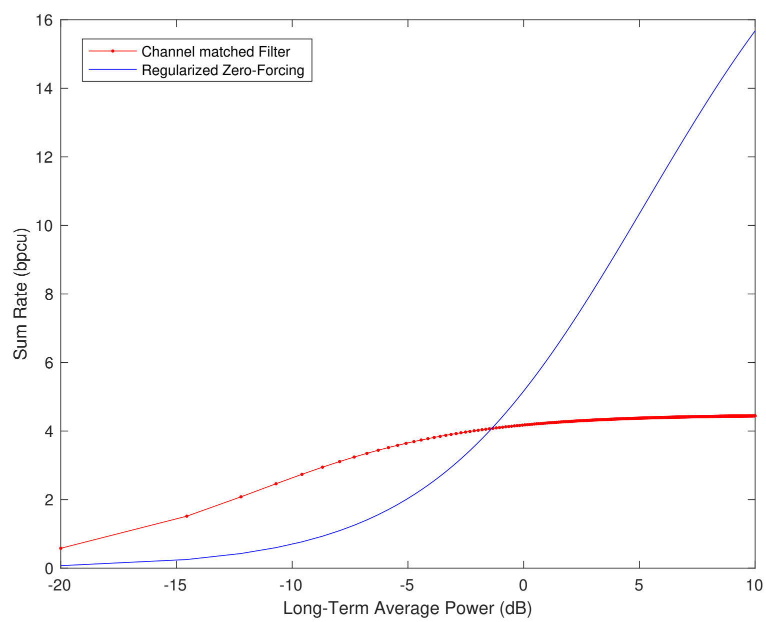

FIGURE 33: Achievable rate for $K = 15$ users in a correlated-tap channel with correlation parameter among antennas $a = 0.99$.

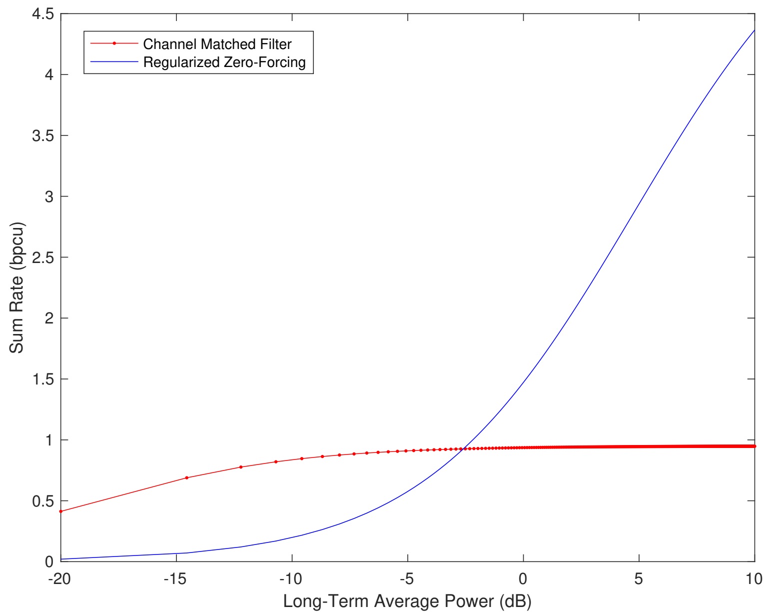

FIGURE 34: Sum-rate of the channel matched filter and regularized zero-forcing for $K = 10$ users in a channel with correlated taps and $a = 0.99$.

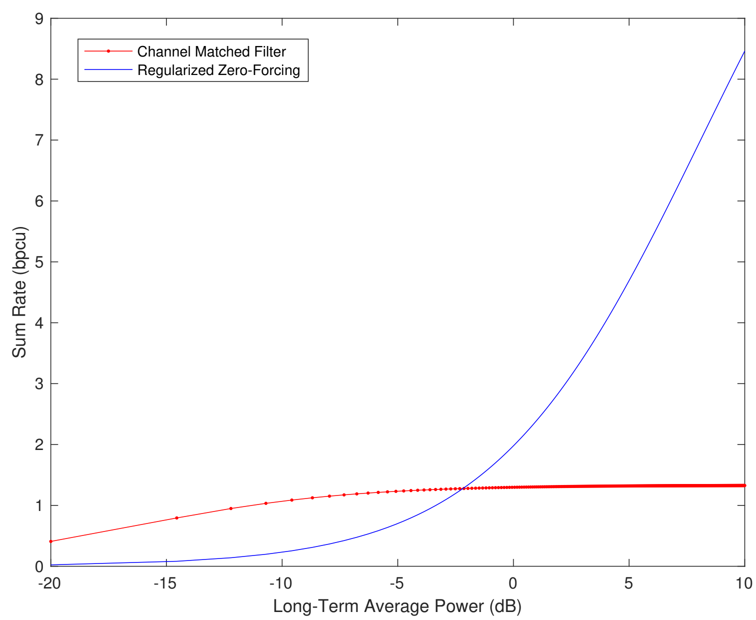

FIGURE 35: Achievable rate for $K = 15$ users in a channel with correlated taps and $a = 0.99$.

Bibliography

[1] A. Pitarokoilis, S. K. Mohammed, and E. G. Larsson, "On the Optimality of Single-Carrier Transmission in Large-Scale Antenna Systems", In: *IEEE Wireless Communication Letters*, Vol. 1, No. 4, pp. 276-279 August 2012.

[2] C. Mellon, E. G. Larsson, and T. Eriksson, "Waveforms for the Massive MIMO Downlink: Amplifier Efficiency, Distortion and Performance", In: *IEEE Transaction on Communications*, Vol. 64, No. 12, pp. 5050-5063 December 2016.

[3] S. Rangan, T. S. Rappaport, and E. Erkip, "Millimeter Wave Cellular Wireless Networks: Potentials and Challenges", In: *Proceedings of the IEEE*, Vol. 102, No. 3, pp. 366-385 March 2014.

[4] S. Buzzi, C. D'Andrea, T. Foggi, A. Ugolini, and G. Colavolpe, "Spectral Efficiency of MIMO Millimeter-Wave Links with Single-Carrier Modulation for 5G Networks", In: 20^{th} *International TIG Workshop on Smart Antennas*, (WSA 2016).